Organic Frameworks for Novel Cobalt Glyoximes as Potential Hydrogen Catalysts

by

Corbin Daniel Ester

Senior Honors Thesis

Appalachian State University

Submitted to the A.R. Smith Department of Chemistry
and the Honors College
in partial fulfillment of the requirements for the degree of

Bachelor of Science

May, 2015

Approved by:

Dale E. Wheeler, Ph.D., Thesis Director

Michael Hambourger, Ph.D., Second Reader

Gregg Marland, Ph.D., Third Reader

Libby G. Puckett, Ph.D., Departmental Honors Director

Leslie Sargent Jones, Ph.D., Director, Honors College

Abstract

The environmental and social implications of global carbon emissions require a rapid transition to alternate energy sources. Cost-effective catalysts for the interconversion of electrical and chemical energy could enable the widespread acceptance of existing renewable energy technologies. In particular, the production of hydrogen via water electrolysis is a promising method of renewable energy storage. Traditional electrolyzing catalysts are either inefficient or require rare, expensive elements. For the hydrogen evolution half-reaction, cobaloximes are active catalysts containing only Earth-abundant, inexpensive elements. The goal of the current research is to synthesize a ligand environment that favors appropriate metal-proton bond strength for catalysis. First, experiments showed that an electron donating N-alkyl side chain cobaloxime enabled catalysis at a lower reduction potential and more basic solvent environment. Compared to the more common glyoxime ligands, such as methyl or phenyl, the introduction of amidoxime functionalities increases the electron density on the central cobalt ion. This demonstrated that changing the electron donating/withdrawing properties of the side chain is an effective way of tuning the redox properties of the cobalt ion. Further research investigated *p*-aniline substituted glyoxime ligands that enable the shift of cobalt-based redox processes to more negative potentials, increasing the accessible pH range of the cobaloxime catalyst. To create these glyoxime derivatives, several *p*-substituted anilines, *p*-$XC_6H_4NH_2$, were used, including X= NO_2, OR, R, H, I, and $N(CH_3)_2$. These N-alkyl and N-aryl glyoximes were analyzed by NMR, IR, and elemental analysis. The corresponding cobaloxime derivatives were then synthesized and analyzed via FTIR, NMR, UV-visible, and MALDI-MS. The results of these efforts will be discussed, although successful synthesis of new glyoxime derivatives and corresponding cobaloximes is still in progress.

Acknowledgements

First I would like to acknowledge first and foremost Dr. Dale E. Wheeler for his guidance, mentorship, and support of this project. I would also like to thank Drs. Mike Hambourger and Gregg Marland for their support and guidance. Furthermore, I would like to thank Katarina Hauser, previous student of Hambourger Lab, and Zach Gilbert, previous student of the Wheeler lab, for their collaboration and work on this project. I would also like to thank the A.R. Smith Department of Chemistry and all of those associated with it for their support. Finally, I would like to thank my family for their unwavering support throughout my academic career.

Table of Contents

List of Figures

List of Tables

List of Abbreviations

cobaloximes	cobalt bis(glyoxime) complexes
$Co(dNhgBF_2)_2$	bis(difluoroboryl(bis(N-*n*-hexyl)glyoxime))cobalt(II)
	N-*n*-hexyl cobaloxime
$Co(dmgBF_2)_2$	bis(difluoroboryldimethylglyoxime)cobalt(II)
	methyl cobaloxime
$Co(dpgBF_2)_2$	bis(difluoroboryldiphenylglyoxime)cobalt(II)
	phenyl cobaloxime
dmg	dimethylglyoxime
dNhg	bis(N-*n*-hexyl)glyoxime
dpg	diphenylglyoxime
bag	bis(N-aniline)glyoxime

List of Synthesized Structures

Series A

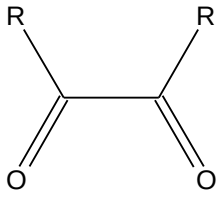

R= 1, 2, 3

1

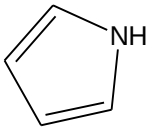

2

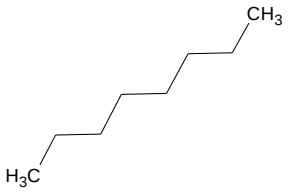

3

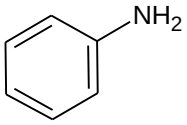

Series B

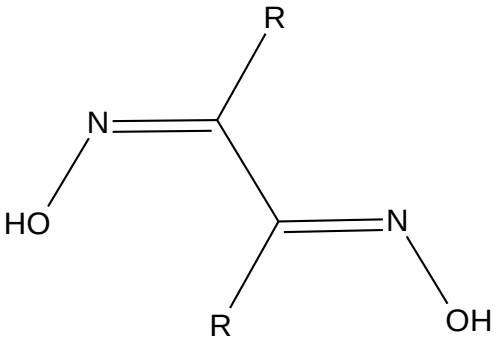

R = 1, 2, 3, 4, 5

1

2

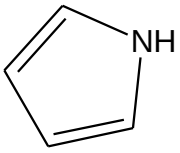

3

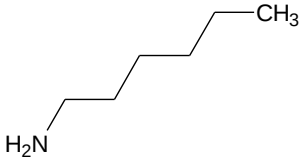

4

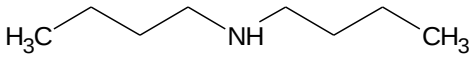

5

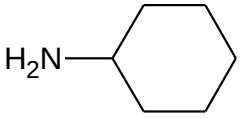

Series C

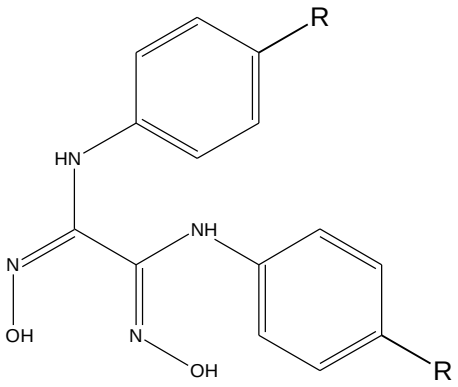

R=1, 2, 3, 4, 5

1 H

2 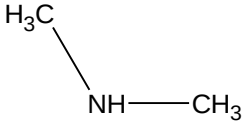

3 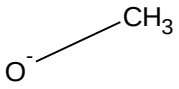

4 Cl^-

5 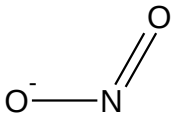

Series D

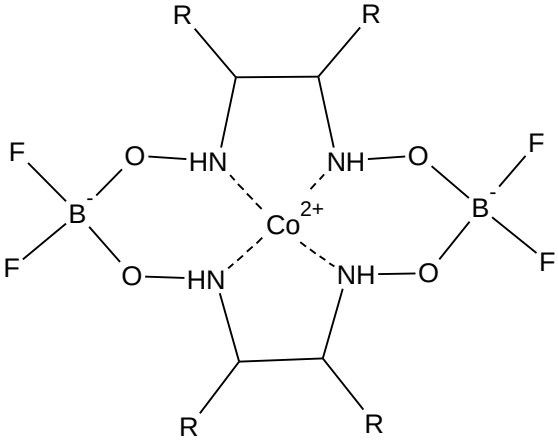

R=1, 2, 3, 4

1 CH_3

2 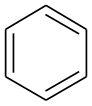

3 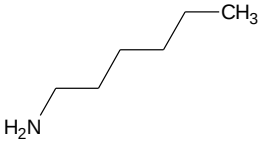

4 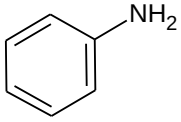

Introduction

International energy consumption has increased quickly over the past few decades, and is predicted to continue to increase at a rate of about 1.5% per year.[1] According to the *International Energy Outlook 2013* (IEO2013), projections hold that the world energy consumption will grow by 56% between 2010 and 2040, see Figure 1.[1] Current total primary energy consumption is at 5.53 x 10^8 terrajoules (TJ) per year, with the United States being responsible for 1.00 x 10^8 TJ alone, a total of 18%. In the United States in 2012, more than 82% of the total marketed energy was obtained from fossil fuels: 36.6% from petroleum and other liquids, 27.3% from natural gas, and 18.3% from coal. Most important is the fact that only 9.0% of this total energy was obtained from renewable resources (see Figure 1)[1, 2].

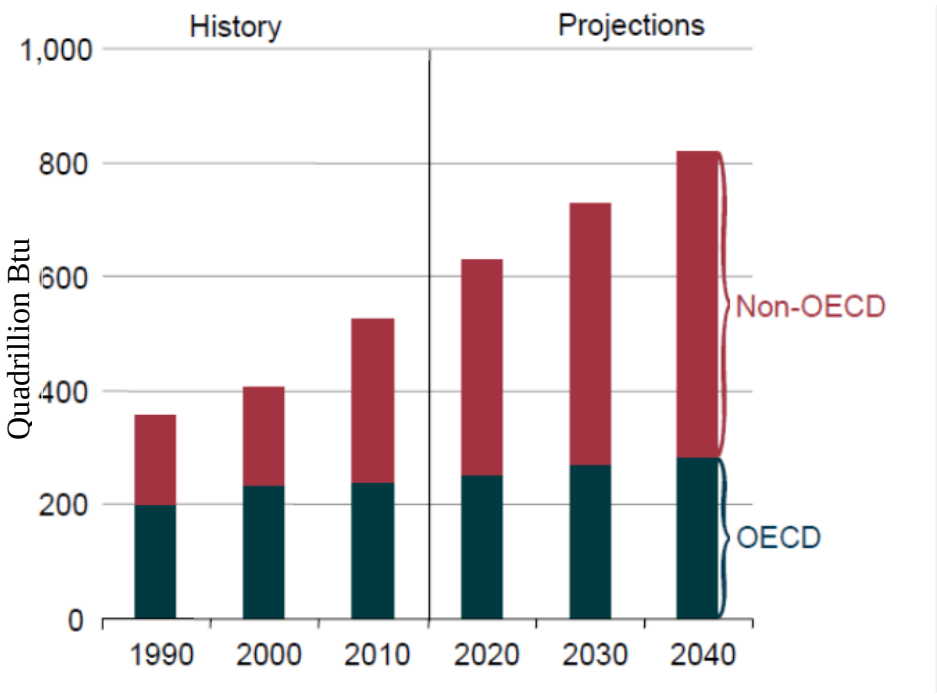

Figure 1: Annual world energy consumption, 1990-2010 and projected to 2040. OECD = Organization for Economic Cooperation and Development. Figure is from the U.S. Energy Information Administration.[1] [1 quadrillion BTU = 1.06 x 10^6 terrajoules].

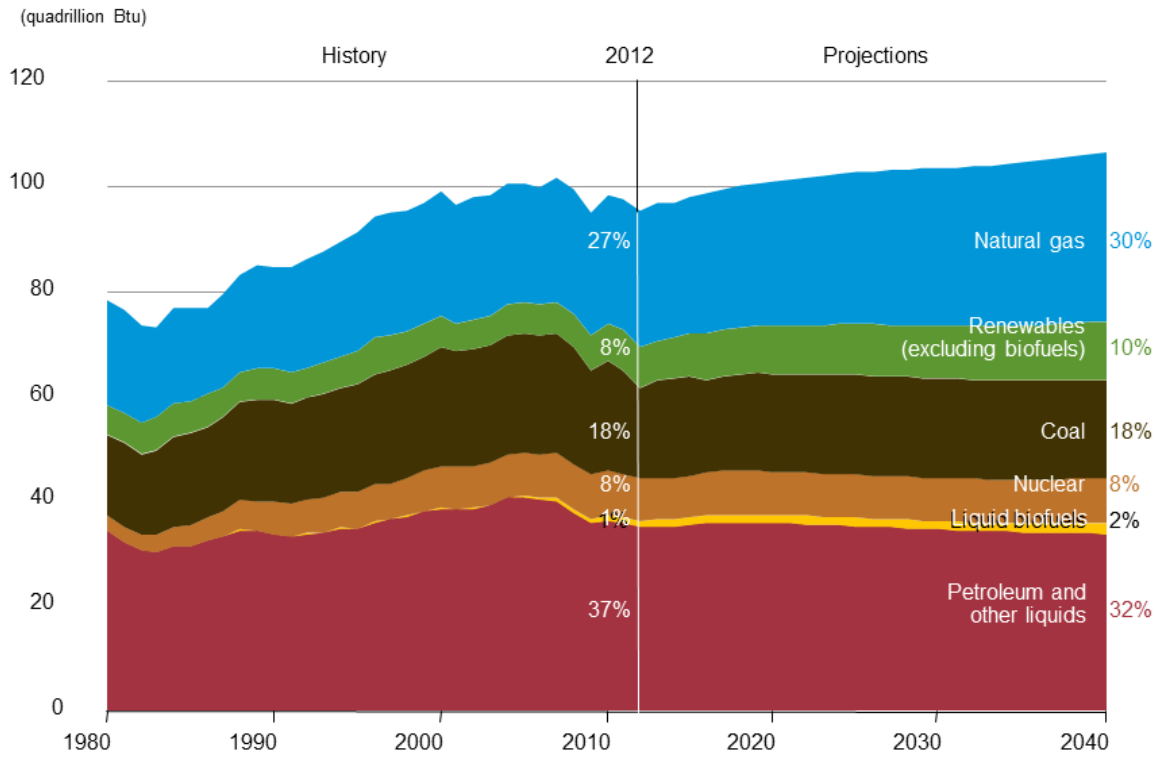

Figure 2: Primary energy consumption in the United States from 1980 – 2040 by energy source. Percentages from 2012 - 2040 are predictions based on current usage. Figure is from the U.S. Energy Information Administration. [1] [1 quadrillion BTU = 1.06 x 10^6 terrajoules].

There are at least nine categories of energy that can be listed for the existing economy: fossil fuels, wind, photovoltaics, solar thermal, hydroelectricity, biomass, geothermal, tidal, and nuclear. Fossil fuels and four of the five most common renewable sources of energy: biomass, water, geothermal, wind, and solar thermal are all ultimately converted solar energy. [3] Solar energy reaches the Earth's surface at an annual average rate of approximately 120,000 TW, which means that in approximately 75 minutes the sun supplies as much energy as the total global marketed energy used in one year.[2, 4] While life on Earth is sustained through the power of the sun, the use of ancient solar energy that has been stored for thousands of years in the form of fossil fuels is finite and its use is placing an undue burden on the global climate.

Although fossil fuels have been an economically viable source of commercial energy, there is an inherent limit to a non-renewable resource that is being used at an increasing rate by a growing population. Furthermore, combustion of these fossil fuels leads to the release of greenhouse gases that compromise the stability of the global climate.[5] Therefore, it is imperative that alternative, renewable sources of energy that effectively harness the power of the sun are sought out in an effort to sustain growing energy demands while mitigating the adverse effects of the current energy infrastructure.[6]

Another advantage of renewable resources is the wide distribution and availability, unlike for fossil fuels. However, some of the most abundant renewable resources (such as wind, solar thermal, and photovoltaics) provide discontinuous supply, and thus research applications are focused on developing means for the inexpensive, efficient storage of energy.[2]

A prime example is using a chemical fuel, such as hydrogen, which can be stored for later oxidation with the concomitant release of energy.[3, 6] However, at present most of the hydrogen fuel is generated during production of fossil fuels for industrial use and so its present use is not addressing the overall concern.[7] The ultimate goal with hydrogen fuel is to first use alternative, renewable energy sources to produce it, and then store it cheaply until use. Electrolysis using renewable electricity and photolysis using discrete molecular systems are two approaches for sustainable hydrogen production.

Electrolysis, see Figure 3, is a well-studied process but the most efficient systems use catalysts derived from elements that are not abundant and therefore, exorbitantly expensive[8]. Hydrogen production is most efficient with the use of a noble metal catalysts such as platinum, a rare, expensive metal that would limit the scalability of the technology.[9] However, any number of inexpensive metallic conductors can be used, such as steel or graphite. [10] While

affordable, these materials offer poor electrode kinetics and therefore operate at large overpotentials and low efficiencies. Water is abundant and chemically stable, making it an ideal electron source for the production of chemical fuels.[12] The ideal catalysts are ones that are highly efficient, low cost, and optimized for stable operation in an aqueous environment.[9, 11]

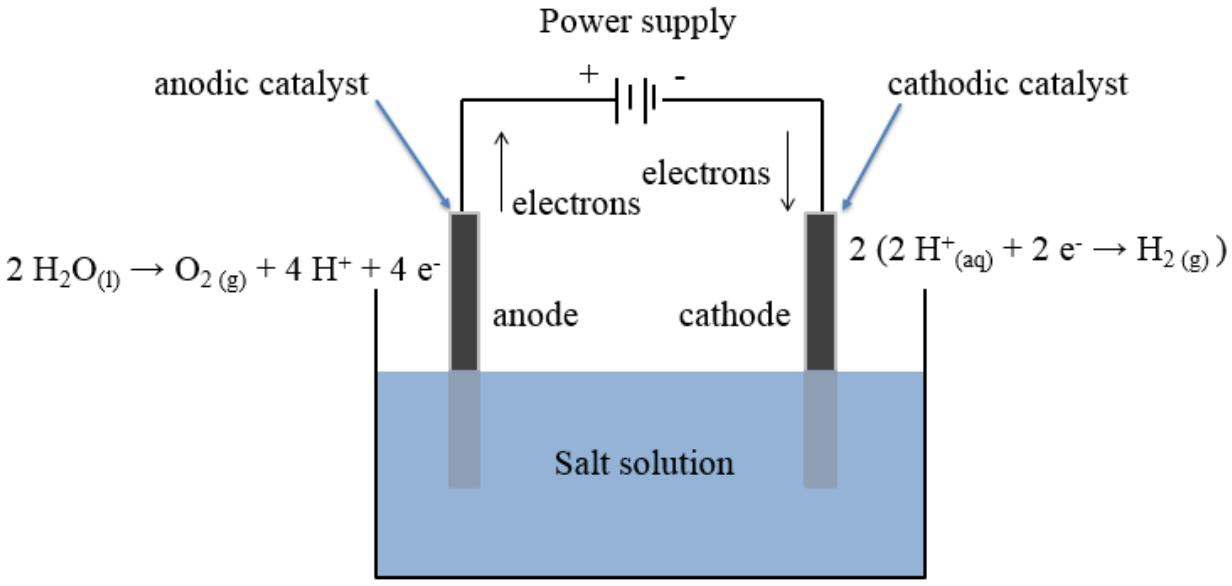

Figure 3: General schematic for the electrolysis of water. Adapted from reference 13.

Overall equation: $2\ H_2O_{(l)} \rightarrow 2\ H_{2\ (g)} + O_{2\ (g)}$.

In natural photosynthesis, see Figure 4, solar energy drives a series of dark electron transfer reactions in Photosystem II (PSII) that leads to the splitting of H_2O into two protons and oxygen. The protons released drive the ATP synthase, and react with NADP to form NADPH, allowing for sugar production. Artificial photosynthesis is a research effort in applying the basic concepts and photochemistry of natural photosynthesis to synthetic systems in order to achieve conversion of solar energy to chemical energy. Research into catalyst

development is a key area for progress toward this goal. Molecular catalysts developed for electrolysis could be readily adapted to photochemical systems.

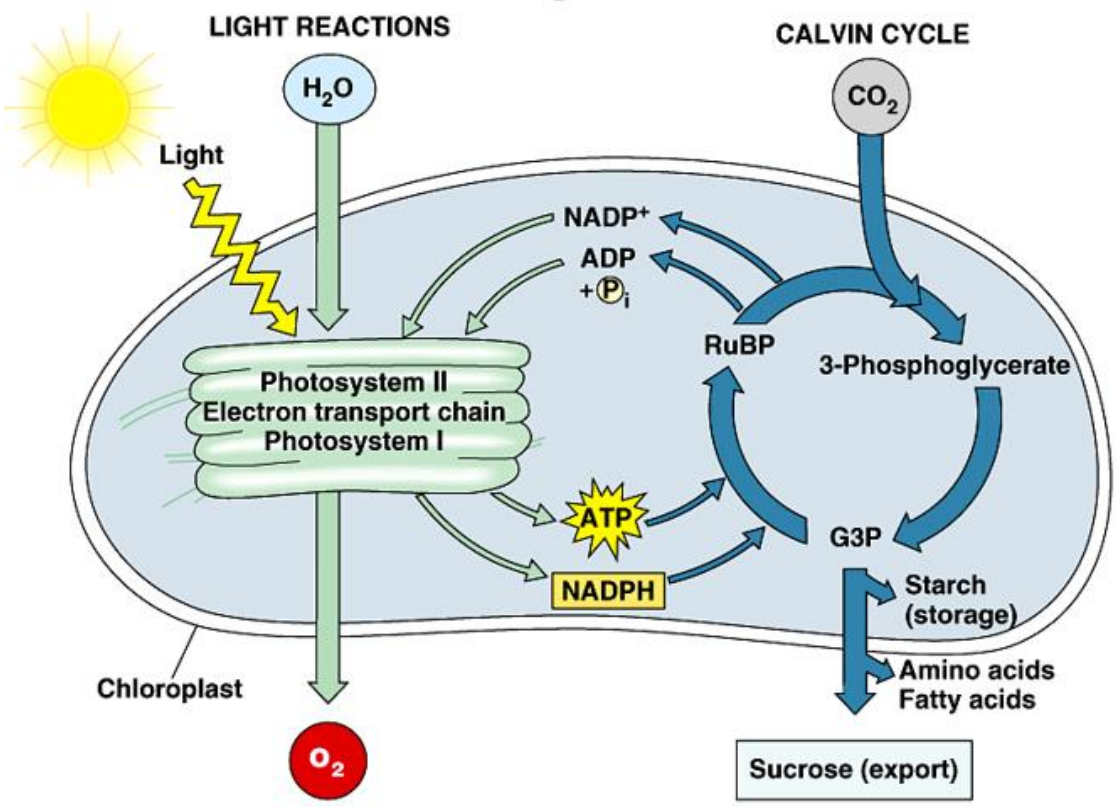

Figure 4: General diagram of oxygenic photosynthesis. Adapted from Campbell Biology.[14]

Overall equation: $6H_2O + 6CO_2 + \text{light} \rightarrow C_6H_{12}O_6 + 6O_2$.

Either electrolysis or photolysis of water requires both a water oxidation and a hydrogen production catalyst. Since the development of a viable water oxidation catalyst has proved to be a more difficult challenge,[15] our current focus is the development of hydrogen production catalysts. There are several promising catalysts for hydrogen production comprised of Earth-abundant materials. These could potentially become viable options for hydrogen production on a global scale. One biological model for identifying promising inorganic catalysts is provided by the hydrogenase enzymes, which are biological catalysts that use either

a [NiFe] or [FeFe] active site to interconvert between molecular hydrogen and protons.[16-17] These catalysts are specifically exciting due to evidence of catalytic activity comparable to platinum using base metals.[18-19] However, with rare exceptions, hydrogenases offer poor stability, especially in the presence of oxygen and/or in the absence of biological repair mechanisms. Small molecule mimics of the hydrogenase enzymes have been pursued in the hopes of emulating their outstanding catalytic activity with a more stable inorganic construct.[20-22]

One particularly promising and economically scalable family of hydrogenase mimics are the cobalt bis(glyoxime) complexes (a.k.a. cobaloximes).[10] Cobalt is an abundant metal and provides promising catalysts that mimic hydrogenases or platinum in a more stable or less expensive system.[10, 23-27] Initial cobaloxime synthesis papers were published in the 1970s, and further research in the 1980s focused on cobaloxime synthesis due to its ability to produce hydrogen gas under acidic aqueous conditions.[28] Attention to these compounds as H_2 catalysts have really have grown since 2005. [10, 29-34]

To be able to understand how to develop cobaloximes adapted for H_2 production in the aqueous environment, it is crucial to understand the mechanism of catalysis. There are two homolytic (bimetallic) and three heterolytic (monometallic) mechanisms proposed to describe the catalytic cycle in which production of hydrogen gas occurs via cobalt(II) complexes. In the two homolytic mechanisms either two cobalt(III)-hydrides react to form cobalt(II) and H_2, or, two cobalt(II)-hydrides react to form two cobalt(I) and H_2, see mechanisms 1 and 2 in Figure 5.[10] However, theoretical calculations predict the second homolytic pathway is not as favorable as the first pathway.[34-35]

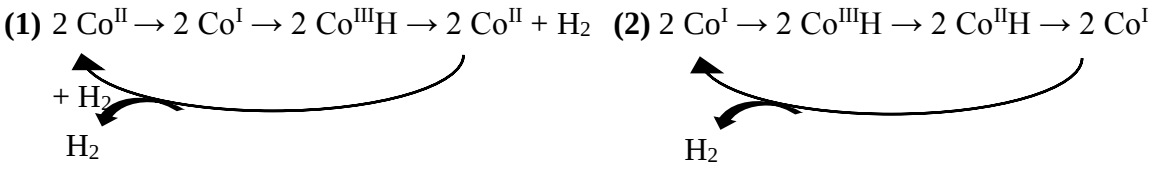

Figure 5: Homolytic H_2 evolution mechanisms. Mechanism 1 is followed by mechanism 2.

In the first heterolytic mechanism, cobalt(II) is reduced to cobalt(I) and then protonated to form a cobalt(III)-hydride, which then reacts with acid to release H_2 and generate cobalt(III), which is reduced back to cobalt(II) to finish the mechanism. In the second heterolytic mechanism, cobalt(III)-hydride can be further reduced to cobalt(II)-hydride, which then behaves like the first mechanism, see mechanisms 3 and 4 in Figure 6, below.[34] The third heterolytic mechanism occurs through reduction of the cobalt(I) species to the cobalt(0) state, followed by protonation to form cobalt(II)-hydride, see mechanism 5 in Figure 6.[10, 34, 35]. Theoretical calculations have shown that the fourth mechanism is thermodynamically favored for $Co(dmgBF_2)_2$.[35]

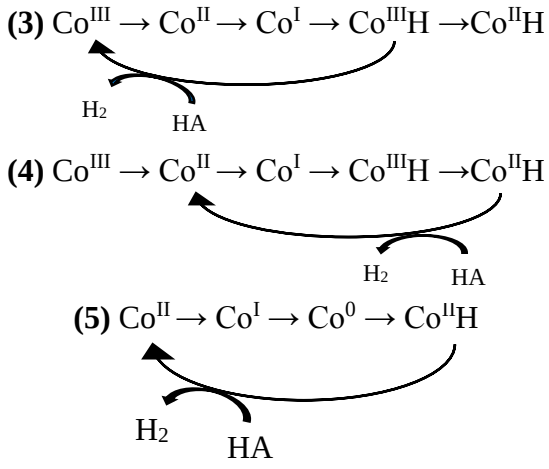

Figure 6: Representation of heterolytic H_2 evolution pathways in acidic environments. Mechanisms proceed in order from 3-5, top to bottom.

While multiple mechanisms have been proposed for catalytic hydrogen production using cobaloxime catalysts, it is not clear that a single mechanism predominates under all solvent conditions. The mechanism of the catalytic cycle likely depends on the acidity of the solvent and the potential of the cobaloxime.[29, 34, 36-38] The more basic (electron rich) cobalt centers presumably proceed more readily through mechanism 3.[38] The less basic cobalt centers proceed through mechanism 5.[29] Furthermore, two identical cobaloximes could theoretically proceed through any of the mechanisms, but mechanism 3 is preferred for more acidic solvents, and mechanism 5 is preferred for less acidic solvents.[36]

Changes to the cobaloxime structure can change the catalytic activity. For example, BF_2 capping groups are typically added to improve the stability of the complex in acid, see Figure 7.[10] This modification improves the stability of the molecule, but also withdraws electron density from the central cobalt ion, requiring more acidic conditions for catalysis to proceed. [10, 33, 36, 40]

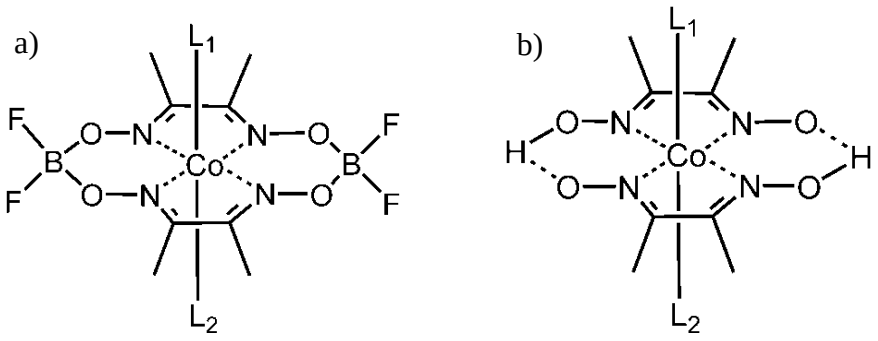

Figure 7: Methyl cobaloxime with bridging groups: (a) BF_2^+ and (b) H^+.

Axial ligands are shown as L_1 and L_2.

Substituents on the glyoxime ligand also can serve to modify the electron density on the cobalt center, thereby changing the acidity of the solvent required to drive catalytic turnover. Two well studied cobaloximes, $Co(dpgBF_2)_2$, and $Co(dmgBF_2)_2$, see Figure 8, are

different in that the methyl groups (Figure 8a) in the first catalyst are more electron donating than the phenyl groups (Figure 8b). As a result, the cobalt center is more electron rich in the methyl derivative. Increase in electron density at the cobalt ion in the methyl derivative increases basicity of the Co(I) state, shifting the cobalt(II) to cobalt(I) couple to a less positive reduction potential, since it is harder to add an electron to the metal center with an increase in electron density at the central atom.

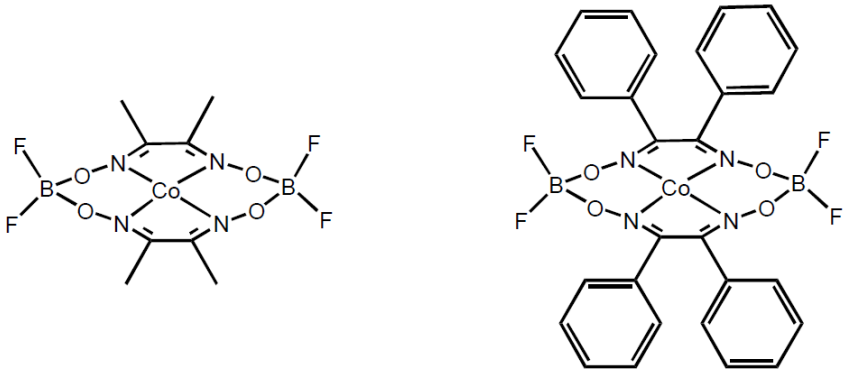

Figure 8: Methyl cobaloxime, $Co(dmgBF_2)_2$, and phenyl cobaloxime, $Co(dpgBF_2)_2$.

Cobaloximes have been demonstrated to produce hydrogen from water or a water/acetonitrile mixture at a pH of less than 4.5.[10, 43] Since this pH is much lower than that of neutral water, efforts are being made to modify the complex to permit rapid catalysis at around pH 7. Studies have shown that catalysis occurs from following protonation of either cobalt(I) or cobalt(0) oxidation states. [10, 30, 36, 39] The basicity of the central atom determines how strongly the cobalt center binds a proton, forming the cobalt hydride. The pH of the solvent environment determines the catalytic turnover rate, and a lower pH is required with a more basic central atom.[37, 41-43] Electron withdrawing and electron donating substituents decrease and increase the basicity of the central atom, respectively. Although recent experiments

provided evidence that catalytic turnover can occur in a 50:50 mixture of water/acetonitrile, the cobaloxime utilized was the more basic but less stable $Co(dmgH)_2$.[40] The more stable $Co(dmgBF_2)_2$ was only catalytically active at pH < 4.5.[43] Therefore, the majority of the cobaloxime research has been conducted using acidified, organic solvents.[10]

Through collaboration with Dr. Hambourger, the goal of this work was to synthesize a novel glyoxime and corresponding cobaloxime that would have increased basicity on the central atom, thereby shifting the cobalt(II) to cobalt(I) reduction potential lower, allowing catalysis more readily in a higher pH environment than the usual low pH organic solvents. To these end, N-*n*-hexylamine, the N-cyclohexylamine, and the N,N-dibutylamine glyoxime derivatives were synthesized. Subsequent reaction of these glyoximes to yield the new BF_2-capped cobaloximes, $Co(dNhexgBF_2)_2$, $Co(dNcyhexgBF_2)_2$, and $Co(dNNdibutgBF_2)_2$, was attempted. Analysis of $Co(dNhexgBF_2)_2$ indicated a cathodic shift in the cobalt(II) to cobalt(I) redox couple of ~1 V. This shift was greater than the expected optimal reduction potential to reduce protons to molecular hydrogen at neutral pH.

After analysis of the N-alkyl glyoxime showed that increased electron density on the central cobalt ion shifted the reduction potential of the cobalt(II) to cobalt(I) couple much more than was needed to drive hydrogen evolution at neutral pH, it became clear that fine-tuning of the ligand was the next step in attempting neutral pH water electrolysis through a cobaloxime. To this end, synthetic efforts were refocused from N-alkyl glyoximes to *p*-aniline glyoximes. First, aniline has delocalized electron density throughout the phenyl ring, which decreases the electron donating effects as compared to alkylamines. Second, changing the *p*-substituent on aniline allows for variation in the electron donating effect of these ligands. Therefore, the

ligand could be tuned to optimize the electron density on the central cobalt ion, influencing the basicity of the cobalt(I) state and enhancing the catalytic activity of the cobaloxime.

To create these new glyoxime derivatives, several *p*-substituted anilines, *p*-$XC_6H_4NH_2$, were used, including X = NO_2, OR, R, H, Cl, and $N(CH_3)_2$. These and all previous ligands were characterized by NMR, IR, UV-visible, and MS, and the resultant cobaloximes were characterized by IR, UV-visible, MS, and magnetic susceptibility. The results and analysis show successful synthesis of several glyoximes and cobaloximes.

Methods

Reagents

Oxalyl chloride (CAS# 79-37-8), anhydrous acetonitrile (CAS# 75-05-8), anhydrous ethanol (CAS# 64-17-5), aniline (CAS# 62-53-3), *n*-hexylamine (CAS# 111-26-2), dibutylamine (CAS# 111-92-2), cyclohexylamine (CAS# 108-91-8), 4-nitroaniline (CAS# 100-01-6), 4-chloroaniline (CAS#106-47-8), N,N-dimethylaniline (CAS# 121-69-7), and *p*-anisidine (CAS# 104-94-9) were purchased from Aldrich (Missouri, US). Diphenylglyoxime was purchased from MP Biomedical (California, US, CAS# 23873-81-6). Dimethylglyoxime (CAS# 95-45-4), boron trifluoride diethyl etherate (CAS# 109-63-7), diethyl ether (CAS# 50-29-7), were purchased from Alfa Aesar (Massachusetts, US). Dichloromethane (CAS# 75-09-2) was purchased from Mallinckrodt (Dublin, Ireland). Cobalt(II) acetate was purchased from Fisher Scientific (Massachusetts, US, CAS# 6147-53-1). Unless otherwise noted, all reagents were used as received without further purification.

Synthesis Procedures

Synthesis procedures were carried out under a dry nitrogen atmosphere with glassware fitted with Teflon solvent seal connections using standard Schlenk techniques.[44] Aniline, *n*-hexylamine, dibutylamine, and cyclohexylamine, were distilled prior to use. *p*-Anisidine was recrystallized from DI water prior to use. Anhydrous ethanol, dichloromethane, chloroform, and anhydrous acetonitrile were used without further purification. All attempted syntheses are labeled with a letter and corresponding number, and the structure of the compound can be found in the list of synthesized structures (pgs. 6-7). Previously reported compounds have CAS

#s indicated in [ ]. All percent yields listed are calculated as a percent of the total yield obtained over the expected theoretical yield of the product predicted. In the glyoxime syntheses, the dichloroglyoxime is the limiting reagent; in the cobaloxime synthesis, the cobalt(II) acetate is the limiting reagent.

A-1: 1,2-Bis (1H-pyrrol-2-nyl)-ethanedione [643-78-7]

The attempted synthesis of this dione follows the modified procedure by Black *et al.*[45] Dry pyridine, freshly distilled pyrrole, and oxalyl chloride were combined in dichloromethane chloride under an N_2 atmosphere at -84 ˚C. The product was washed with 5M HCl, extracted with dichloromethane, neutralized with $NaHCO_3$, and dried over anhydrous $MgSO_4$ and Na_2CO_3. The product was purified using hexane/acetone on a silica gel column. The solvents were removed using a rotary evaporator. No evidence of product formation was found.

A-2: Dioctyl ethanedioate [20760-45-6]

The attempted synthesis of this dione follows the modified procedure by Black *et al.*[45] Freshly distilled 1-octanol (2.38 g, 18.28 mmol) and oxalyl chloride (1.05 g, 8.27 mmol) were combined in dichloromethane under an N_2 atmosphere at -84 ˚C. This reaction was slowly warmed to room temperature and stirred for 48 hours. The mixture was washed 3 times with NaCl solution and dichloromethane, and the organic layer was dried over anhydrous $CaCl_2$. After drying under vacuum for 48 hours, the resultant substance was oily and white. NMR analysis showed a predominate presence of the starting material, 1-octanol. No evidence of product formation was found.

A-3: N1,N2-Diphenylethanediamide [620-81-5]

The attempted synthesis of this dione follows the modified procedure by Black *et al.*[45] Freshly distilled aniline (4.76 g, 51.2 mmol) and oxalyl chloride (3.0 g, 23.6 mmol) were combined in dry tetrahydrofuran under an N_2 atmosphere at 0°C, immediately producing a white solid in a tan solution. The solvents were removed using a rotary evaporator. No evidence of product formation was found.

B-1: Dichloroglyoxime [2038-44-0]

This synthesis follows a modified procedure by Lance *et al.*[46] Into two reaction flasks separately were added glyoxal sodium bisulfite (20.0 g, 70.0 mmol), hydroxylamine hydrochloride (10.0 g, 144.0 mmol), and K_2CO_3 (20.0 g, 145.0 mmol). The reactants were suspended in methanol (500 mL) and stirred under reflux overnight, producing dark brown solutions containing a lighter brown suspended solid. The suspensions were filtered while hot through a Celite pad on a glass frit, producing a slightly brownish/reddish solution. The total volume of solution (1100 mL) was reduced to ~50 mL using a rotary evaporator, then stored at 4°C under reduced pressure. The brown precipitate was filtered and dissolved in hot DI water in a 500 mL side arm flask. To the aqueous brown solution (175 mL), concentrated HCl (43 mL) was added producing a lighter brown solution. The solution was placed on ice and stirred moderately as Cl_2 gas was bubbled through the reaction. After 1.5 hrs, a yellow solution with a clean white precipitate was visible. The white solid was collected by vacuum filtration, and washed with DI water (100 mL). Yield: 2.529 g, 23.1%. IR ($\bar{\upsilon}_{max}/cm^{-1}$): 3240 (OH), 1409 (C═N), 1000 (N-O); ^{1}H-NMR δ_H ($CDCl_3$): 13.17 (s, 2H, NOH) ppm; ^{13}C-NMR δ_C ($CDCl_3$): 131.4 (C=N-O ppm.

B-2: 1,2-Bis(1H-pyrrol-2-nyl)-ethanedioneglyoxime [138556-59-9]

The attempted synthesis of this glyoxime followed the modified procedure of Kim *et al.*[47] The 1,2-Bis(1H-pyrrol-2-nyl)-ethanedione (0.075 g, 0.384 mmol) was dissolved in ethanol. An excess of K_2CO_3 (0.165 g, 1.19 mmol) and hydroxylamine hydrochloride (0.272 g, 3.91 mmol) were added. The solution refluxed for 3 days. The precipitate was collected and washed with cold water. The product decomposed. No evidence of product formation was found.

B-3: Bis(N-*n*-hexyl)glyoxime [681431-95-8]

This synthesis is a modified procedure from Gümüs, *et al.*[48] *n*-Hexylamine (1.29 g, 12.8 mmol) was dissolved in anhydrous ethanol (6.45 mL) under dry N_2. A solution of dichloroglyoxime (0.500 g, 3.19 mmol) in anhydrous ethanol (12.9 mL) was added dropwise and the solution immediately turned yellow. The reaction mixture was stirred at room temperature (~ 20 ^oC) overnight. The product was extracted from the reaction mixture using hexanes/DI water. The yellow hexane layer was dried over $CaCO_3$ and filtered. The hexanes were removed under vacuum yielding dNhg. Yield: 0.775 g, 84.8%. IR ($\bar{\upsilon}_{max}/cm^{-1}$): 3410 (NH), 3240 (OH), 2960, 2930, and 2860 (CH_2), 1660 (C═N), 910 (N-O); ^{1}H-NMR δ_H ($CDCl_3$): 8.66 (broad s, 2H, NOH), 5.08 (s, 2H, NH), 3.04 (q, 4H, N-C*H*$_2$), 1.45 (m, 4H, N-CH_2-C*H*$_2$), 1.24 (s, 12H, CH_2), 0.84 (t, 6H, CH_3) ppm; ^{13}C-NMR δ_C ($CDCl_3$): 147.82 (C=N-O), 43.21 (N-*C*H_2), 31.68 (N-CH_2-*C*H_2), 31.06 (CH_2), 26.52 (CH_2), 22.70 (CH_2), 14.14 (CH_3) ppm. Anal. Calcd: C, 58.71; H, 10.56; N, 19.56. Found: C, 58.6 ± 0.5; H, 10.9 ± 0.1; N, 18.6 ± 0.3.

B-4: Bis(N,N-dibutyl)glyoxime [Not previously reported]

This synthesis is a modified procedure from Gümüs, *et al.*[48] Dibutylamine (1.98 g, 15.3 mmol) was dissolved in absolute ethanol (9.0 mL) under dry N_2. To this solution, dichloroglyoxime (0.600 g, 3.82 mmol) in absolute ethanol (15.0 mL) was added dropwise. Upon addition, a color change to dark yellow was immediately observed. The mixture was heated to 45°C for 4 hours, after which the solution was pale yellow and opaque. This solution was stirred for 24 hours at room temperature. DI water (50 mL) was added, first precipitating a white solid, then producing yellow oily globules in the solution. Gravity filtration yielded the yellow oily product, which was washed five more times with DI water. Residual solvent was removed from the oily yellow layer under reduced pressure, producing a yellow solid. Yield: 1.064 g, 55.0%. IR ($\bar{\upsilon}_{max}/cm^{-1}$): 3284 (OH), 2956, 2929, and 2863 (CH_2), 1620 (C═N), 937 (N-O); ^{1}H-NMR δ_H ($CDCl_3$): 7.69 (broad s, 2H, NOH), 2.98 (t, 8H, N-C*H*$_2$), 1.40 (m, 8H, N-CH_2-C*H*$_2$), 1.17 (m, 8H, CH_2), 0.81 (t, 12H, CH_3) ppm; ^{13}C-NMR δ_C ($CDCl_3$): 153.11 (C=N-O), 48.03 (N-*C*H_2), 29.68 (N-CH_2-*C*H_2), 20.49 (CH_2), 14.15 (CH_3) ppm.

B-5: Bis(N-cyclohexyl)glyoxime [4332-01-8]

This synthesis is a modified procedure from Gümüs, *et al.*[48] Dicyclohexylamine (0.759 g, 7.65 mmol) was dissolved in absolute ethanol (4.5 mL) under dry N_2. To this solution, dichloroglyoxime (0.300 g, 1.91 mmol) in absolute ethanol (7.5 mL) was added dropwise. Upon addition, a color change to yellow-orange was immediately observed. The mixture stirred overnight. The solution was refluxed for 4 hours, turning the solution light yellow and opaque. DI water (24 mL) was added, and an extraction was performed in chloroform. The yellow, organic layer was dried under vacuum and the resulting product analyzed. Yield: 0.515

g, 95.1%. IR ($\bar{\upsilon}_{max}/cm^{-1}$): 3325 (NH), 3258 (OH), 2926 and 2853(CH_2), 1637 (C═N), 933 (N-O); ^{1}H-NMR δ_H ($CDCl_3$): 5.94 (broad s, 2H, NOH), 5.04 (d, 2H, NH), 3.13 (t, 2H, N-C*H*$_2$), 2.61 (m, 4H, N-CH_2-C*H*$_2$), 1.79 (m, 2H, CH_2), 1.63 (m, 2H, CH_2), 1.49 (m, 4H, CH_2), 1.24-1.01 (m, 4H, CH_2), 0.84 (t, 4H, CH_2) ppm; ^{13}C-NMR δ_C ($CDCl_3$): 146.94 (C=N-O), 51.15 (N-*C*H$_2$), 49.89 (N-CH_2-*C*H$_2$), 35.62 (CH_2), 34.93 (CH_2), 25.33 (CH_2), 24.87 (CH_2) ppm. Anal. Calcd: C, 59.55; H, 9.28; N, 19.84. Found: C, 63.4; H, 11.2; N, 16.0.

C-1: Bis(N-aniline)glyoxime [4332-00-7]

This synthesis is a modified procedure from Gümüs, *et al.*[48] To a solution of aniline (0.420 g, 4.51 mmol) in anhydrous ethanol (15 mL), an excess (0.95 g) of solid $NaHCO_3$ was added and stirred for 1 hour. To this clear solution, a solution of dichloroglyoxime (0.348 g, 2.22 mmol) in anhydrous ethanol (10 mL) was added. This solution was stirred at room temperature for 20 hours producing an opaque, yellow solution. Gravity filtration of the solution produced a white solid layer and a clear orange liquid layer. The orange solution was dried under vacuum, leaving a yellow-orange solid after evaporation of the solvent. Trituration in diethyl ether produced a white solid, which was acquired through vacuum filtration. The product is a yellowish-white solid. Yield: 0.294 g, 49.0%. IR ($\bar{\upsilon}_{max}/cm^{-1}$): 3371 (NH), 3038, 2904 and 2778(CH), 1636 (C═N), 971 (N-O); ^{1}H-NMR δ_H (DMSO-d_6): 10.45 (broad s, 2H, NOH), 8.16 (s, 2H, NH), 7.06 (t, 8H, C*H*), 6.08 (t, 12H, *p*-C*H*) ppm; ^{13}C-NMR δ_C (DMSO-d_6): 140.23 (C=N-O), 128.69 (N-*C*H), 121.71 ($CH_)$, 119.38 (*p*-CH) ppm.

C-2: N1,N2-bis[4-(dimethylamino)phenyl]-*N'1,N'2*-dihydroxyethanediimidamide

[Not previously reported]

This synthesis is a modified procedure from Gümüs, *et al.*[48] To a solution of *N*,*N*-dimethylbenzene-1,4-diamine (0.177 g, 1.30 mmol) in anhydrous ethanol (30 mL), an excess of K_2CO_3 (0.440 g, 3.18 mmol) was added and stirred at room temperature for 1 hour producing a dark purple solution. To this solution, a solution of dichloroglyoxime (0.100 g, 0.637 mmol) in anhydrous ethanol (3 mL) was added dropwise. This mixture was stirred at room temperature for 18 hours, then filtered to remove excess K_2CO_3. The deep purple solution was placed under vacuum producing a dark, black, goopy solid. The solid was triturated with diethyl ether and gravity filtered, producing a purple solid. Analysis failed to indicate presence of product.

C-3: N'1,N'2-dihydroxy-N1,N2-bis(4-methoxyphenyl)ethanediimidamide [215934-70-6]

This synthesis is a modified procedure from Gümüs, *et al.*[48] To a solution of *p*-anisidine (0.160 g, 1.30 mmol) in anhydrous ethanol (5 mL) an excess of K_2CO_3 (0.440 g, 3.18 mmol) was added and stirred at room temperature for 1 hour. To this clear solution, a solution of dichloroglyoxime (0.100 g, 0.637 mmol) in anhydrous ethanol (3 mL) was added dropwise. The solution immediately turned rubber yellow. After 4 hours of stirring, the solution turned light brown. The solution was gravity filtered, and the resultant brown liquid was placed under vacuum producing a dark yellow solid. Diethyl ether trituration and subsequent vacuum filtration produced a light brownish solid. Yield: 0.150 g, 71.4%. IR ($\bar{\upsilon}_{max}$/cm^{-1}): 3382 (NH), 3312 (OH), 3004, 2961, 2939, and 2915(CH), 2837 (CH_3), 1504 (C=N), 971 (N-O); ^{1}H-NMR δ_H (DMSO-d_6): 10.13 (broad s, 2H, NOH), 7.84 (s, 2H, NH), 7.19 (m, 8H, C*H*), 6.89

(s, 6H, *CH*$_3$) ppm; ^{13}C-NMR δ_C (DMSO-d$_6$): 154.51 (C=N-O), 143.43 (*C*H), 132.91 (CH), 121.32 (CH), 113.46 (CH), 55.99 (CH$_3$) ppm.

C-4: N1,N2-bis(4-chlorophenyl)-N'1,N'2-dihydroxyethanediimidamide [60035-40-7]

This synthesis is a modified procedure from Gümüs, *et al.*[48] To a solution of 4-chloroaniline (0.166 g, 1.30 mmol) in anhydrous ethanol (5 mL), an excess of K_2CO_3 (0.440 g, 3.18 mmol) was added and stirred at room temperature for 1 hour. The solution immediately turned yellow upon drop-wise addition of dichloroglyoxime (0.100 g, 0.637 mmol) in anhydrous ethanol (3 mL). This mixture was stirred at room temperature for 16 hours. The solution was gravity filtered and placed under vacuum to remove the solvent, producing an orange-yellow solid. Trituration with diethyl ether and vacuum filtration produced a yellowish solid. No evidence of product formation was found.

C-5: [Not previously reported]

1,2-bis(hydroxyimino)ethane-1,2-diyl]bis(iminobenzene-diyl)bis[hydroxy(oxo)ammonium]

This synthesis is a modified procedure from Gümüs, *et al.*[48] To a solution of 4-nitroaniline (0.414 g, 3.00 mmol) in anhydrous ethanol (10 mL) an excess (0.672 g) of $NaHCO_3$, was added and stirred at room temperature for one hour. The solution immediately turned yellow upon drop-wise addition of dichloroglyoxime (0.235 g, 1.50 mmol) in anhydrous ethanol (5 mL). This mixture was stirred at room temperature for 16 hours. The solution was gravity filtered and placed under vacuum to remove the solvent, producing an orange-yellow solid. Trituration with diethyl ether and vacuum filtration produced a yellowish solid. No evidence of product formation was found.

D-3: $Co(dNhgBF_2)_2$

This synthesis is a modified procedure from Tovrog *et al.*[50] To a solution of 52.9 mg (0.185 mmol) of **B-3** in 4.0 mL of hexanes, 25.7 mg (0.103 mmol) of cobalt(II) acetate tetrahydrate was added at 0°C under N_2. Boron trifluoride diethyl etherate (50 μL) was added drop-wise to the solution at 0°C. After 30 minutes the solution was allowed to warm to room temperature and then refluxed for 5 hours. During the 5 hours a red solid formed. Next, the hexanes were removed and the compound dissolved in dichloromethane, washed with DI water, dried over $MgSO_4$ and filtered. The solvent was removed under reduced pressure and the red product was dried in a desiccator. The oily compound was recrystallized repeatedly in a small amount of dichloromethane in hexanes. Yield: 34.7 mg (51.8 %). IR ($\bar{\upsilon}_{max}/cm^{-1}$): 1614 (C═N), 976 (N-O); ^1H NMR ($CDCl_3$): 5.36 (s, 2H, NH), 3.09 (q, 4H, N-C*H*$_3$), 1.52 (m, 4H, N-CH_2-C*H*$_2$), 1.28 (s, 12H, C*H*$_2$), 0.88 (t, 12H, CH_3) ppm.^{13}C NMR ($CDCl_3$): 152.59 (C=N-O), 46.05 (N-*C*H_2), 31.57 (N-CH_2-*C*H_2), 29.94 (CH_2), 26.32 (CH_2), 22.79 CH_2), 14.22 (CH_3) ppm. MALDI-MS (t-BPPM-Matrix); M+Matrix; Expected: 975.5 m/z; Observed: 971.9 m/z. UV-visible: λ_{max}=526 nm.

D-4: $Co(dBagBF_2)_2$

This synthesis is a modified procedure from Tovrog *et al.*[50] A solution of **C-1** (0.150 g, 0.56 mmol) in diethyl ether (5 mL) was put on ice under a flow of N_2 for 15 minutes. Then, cobalt(II) acetate tetrahydrate (0.198 g, 1.12 mmol) was added and the solution stirred under a flow of N_2 for 5 minutes. Boron trifluoride diethyl etherate (0.75 mL) was added dropwise, and N_2 flushed through the system for 5 more minutes, after which the reaction was sealed under N_2 and left to stir at room temperature for 24 hours. The solution was filtered

producing a brownish-red liquid, which produced a dark brown oily solid after removing the solvent by vacuum. This solid was washed and filtered with DI water producing a red-colored aqueous layer. This layer was placed under vacuum again producing a brown solid, which was then run through a hexanes/acetone silica gel column. A reddish-brown layer was recovered from the column and dried under vacuum. Percent yield: 0.063 g, 47.0%. MS=1; UV-visible: λ_{max}=415 nm.

Analytical Procedures

Carbon-Hydrogen-Nitrogen (CHN) Analysis

Compounds were dried under vacuum before analysis. Acetanilide (CAS# 103-84-4, Perkin Elmer, Waltham, MA) was used as the standard for calibration. Samples (3 mg) were introduced to the instrument and combusted in the presence of O_2. Combustion products quantified by gas chromatography with a ± 0.3 % accuracy.

UV-visible spectrophotometry

All UV-visible spectra data were collected via Shimadzu UV-2401 spectrophotometer using a 1 cm path length quartz cuvette. Before measurement, a baseline of neat solvent was recorded. Air was used as a reference sample.

Fourier transform infrared spectrophotometry (FTIR)

FTIR spectral data were collected via Nicolet 550 Magna IR. For each spectrum, the sample was prepared between two KBr plates.

Magnetic Susceptibility

Magnetic susceptibility was determined using an Evans Balance by placing a few mg of sample in the magnetic susceptibility tube and inserting into instrument.

Nuclear magnetic resonance (NMR) spectroscopy

All NMR spectra were collected using a Varian Gemini 2000 NMR or Bruker Ascend NMR spectrometer. Samples were prepared by dissolving ~10 mg in a deuterated solvent.

Cyclic Voltammetry (CV)

All CV work was performed by Katarina Hauser in Dr. Hambourger's lab. CV was performed in a standard three-electrode configuration. The three electrodes, a glassy carbon working electrode, platinum wire counter electrode, and Ag/AgCl reference electrode, were all obtained from BioAnalytical Systems (West Lafayette, IN). Full experimental detail can be found in reference 13.

Results

Characterization of Compounds A1-A3

No evidence was found indicating the successful synthesis of compounds **A-1**, **A-2**, or **A-3**.

Characterization of Compounds B1-B5

Compound **B-1** was characterized via ^{1}H NMR, ^{13}C NMR, and FTIR. Although no evidence was found indicating the successful synthesis of compound **B-2**, compounds **B-3**, **B-4**, and **B-5** were all characterized via ^{1}H NMR (Table 1); ^{13}C NMR (Table 2); and FTIR (Table 3). All NMR and FTIR spectra can be found in Appendices A and B, respectively. ^{1}H and ^{13}C NMR for compounds **B-1**, **B-3**, **B-4**, and **B-5** were all taken with $CDCl_3$ as a solvent.

Furthermore, compounds **B-3** and **B-5** were characterized via elemental analysis. For compound **B-3**, the theoretical percentages for $C_{14}H_{30}N_4O_2$ are 58.71, 10.56, and 19.56 mass percent for C, H, and N, respectively; observed data were 58.6 ± 0.5; 10.9 ± 0.1; and 18.6 ± 0.3, respectively. For compound **B-5**, the theoretical percentages for $C_{14}H_{26}N_4O_2$ are 59.55, 9.28, and 19.84 % for C, H, and N, respectively; observed data were 63.4, 11.2, and 16.0, respectively.

Table 1: ^{1}H NMR and data for **B-1**, **B-3**, **B-4**, and **B-5** with comparable literature values.

Cmpd	**(a) ^{1}H Chemical Shift, ppm (Integration)**		
	(N-OH)	**(N-H)**	**Alkyl/aryl hydrogens (C-H)**
B1	13.17	-	-
B3	8.66 (2)	5.08 (2)	3.04 (4), 1.45 (4), 1.24 (12), 0.84 (6)
B3[48]	8.44 (2)	5.08 (2)	3.09 (4), 1.49 (4), 1.27 (12), 0.86 (6)
B4	7.69 (2)	-	2.98 (8), 1.40 (8), 1.17 (8), 0.81 (12)
B5	5.94 (2)	5.04 (2)	3.13 (2), 2.61 (4), 1.79 (2), 1.63 (2), 1.49 (4), 1.24-1.01 (4), 0.84 (4)

Table 2: ^{13}C NMR and data for **B-1**, **B-3**, **B-4**, and **B-5** with comparable literature values.

Cmpd	**(b) ^{13}C Chemical Shift, ppm**	
	(C-NOH)	**Alkyl/aryl hydrogens (C-H)**
B1	131.4	-
B3	147.82	43.21, 31.68, 31.06, 26.52, 22.70, 14.14
B3 (lit.)[48]	147.98	42.97, 31.51, 30.81, 26.36, 22.55, 13.99
B4	153.11	48.03, 29.68, 20.49, 14.15
B5	146.94	51.15, 49.89, 35.62, 34.93, 25.33, 24.87

Table 3: FTIR peaks for **B-1**, **B-3**, **B-4**, and **B-5** with comparable literature values.

Cmpd	υ_{max}/cm^{-1}				
	NH	**OH**	**CH2**	**C=N**	**N-O**
B1	-	3239	-	1409	1000
B3	3410	3240	2960, 2930, 2860	1660	910
B3 (lit.)[48]	3400	3300	2920, 2850	1650	900
B4	3284	-	2956, 2929, 2863	1620	937
B5	3325	3258	2926, 2853	1637	933

Characterization of Compounds C1-C5

Although no evidence was found indicating the successful synthesis of compound **C-2**, **C-4**, or **C-5**, compounds **C-1** and **C-3** were both characterized via ^{1}H NMR, ^{13}C NMR, and FTIR, see Tables 4, 5, and 6. ^{1}H and ^{13}C NMR for **C-1** and **C-3** were taken in DMSO-d_6.

Table 4: ^{1}H NMR and data for **C-1**, **C-3**, and comparable literature values.

Cmpd	**(a) ^{1}H Chemical Shift, ppm (Integration)**		
	(N-OH)	**(N-H)**	**Alkyl/aryl hydrogens (C-H)**
C1	10.45 (2)	8.16 (2)	7.06 (8), 6.80 (12)
C1 (lit.)[52]	10.41 (2)	8.01 (2)	6.97 (8), 6.71 (12)
C3	10.13 (2)	7.84 (2)	7.19 (8), 6.89 (6)

Table 5: ^{13}C NMR and data for **C-1**, **C-3**, and comparable literature values.

Cmpd	(b) ^{13}C Chemical Shift, ppm	
	(C-NOH)	Phenyl hydrogens (C-H)
C1	140.23	128.69, 121.71, 119.38
C1 (lit.) [52]	140.40	128.86, 121.93, 119.60
C3	143.43	154.51, 132.91, 121.32, 113.46, 55.99 (O-*C*H_3)

Table 6: FTIR peaks for **C-1**, **C-3**, and comparable literature values.

Cmpd	υ_{max}/cm^{-1}				
	NH	OH	CH2	C=N	N-O
C1	3371	-	3038, 2904, 2778	1636	971
C1 (lit.) [52]	3375	3275	3025, 2890-2791	1642	974
C3	3382	3312	3004, 2961, 2939, 2915, 2837	1504	971

Characterization of Compounds D1-D4

Compounds **D1** and **D2** are the two well-known cobaloximes that are most well represented in the literature. During my tenure in the lab, both compounds were prepared, characterized, and studied by other undergraduate researchers in order to assure our ability to prepare this class of compounds.[13] Since the results did not deviate substantially from literature, literature values are reported herein. To this end, the **D-3** synthesis is different from the other three syntheses due to using hexanes instead of diethyl ether as the solvent. While ether was a sufficient solvent system for the other syntheses, the **D-3** compound formed using ether as the reaction solvent decomposed during the water wash, while the product formed in

refluxing hexanes maintained stability during the water wash. For compound **D-4** synthesis, characterization data for the product formed in ether is presented; in the synthesis of **D-3**, the data for the product formed in refluxing hexanes is presented.

The red-brown **D-4** compound was initially characterized by magnetic susceptibility. Compound **D-3** was not characterized with magnetic susceptibility because it was recovered as an oil rather than a powder sample like **D-4**. Magnetic susceptibility was used to determine the number of unpaired electrons, n, in the cobalt complexes. The calculated n for compound **D-4** was 0.67.

Although magnetic susceptibility of **D-3** could not be obtained, a ^{1}H NMR spectrum was obtained. Since paramagnetic compounds widen the peaks in an NMR spectrum, it is not possible to obtain a clean NMR of paramagnetic cobalt(II) complexes. Obtaining a NMR spectrum of the cobaloxime confirmed the presence of diamagnetic cobalt(III) center. See Tables 7 and 8 for a summary of data for the ^{1}H NMR and ^{13}C NMR of **B-3** and **D-3**.

Table 7: ^{1}H NMR data for **B-3** and **D-3**.

Shift (ppm)	**Int.**	**B-3**	**Shift (ppm)**	**Int.**	**D-3**
8.66	2H	NO*H*	-	-	-
5.08	2H	N*H*	5.36	4H	N*H*
3.04	4H	N-CH_2	3.09	8H	N-CH_2
1.45	4H	NCH$_2$-CH_2	1.52	8H	NCH$_2$-CH_2
1.21	12H	CH_2	1.28	24H	CH_2
0.84	6H	CH_3	0.88	12H	CH_3

Table 8: ^{13}C NMR data for **B-3** and **D-3**.

Chemical Shift (ppm)	**dNhg Assignment**	**Chemical Shift (ppm)**	**$Co(dNhgBF_2)_2$ Assignment**
147.82	*C*=N-O	152.59	*C*=N-O
43.21	N-*C*H_2	46.02	N-*C*H_2
31.68	N-CH_2-*C*H_2	31.57	N-CH_2-*C*H_2
31.06	*C*H_2	29.94	*C*H_2
26.52	*C*H_2	26.32	*C*H_2
22.70	*C*H_2	22.79	*C*H_2
14.14	*C*H_3	14.22	*C*H_3

UV-visible spectra of compounds **D-3** and **D-4** were obtained. All UV-visible spectra are shown in Appendix C. UV-visible spectra for **D-3** and **D-4** were obtained in dichloromethane. The experimental λ_{max} for the MLCT band in compounds **D-3** and **D-4** were 526 nm and 415 nm, respectively, see Table 9. Values obtained for **D-1** and **D-2** are a reasonable match to literature values.[38, 53]

Table 9: Experimental λ_{max} for the MLCT band in compounds **D-3** and **D-4**.

Complex	**λ_{max} (nm)**
D-3	526
D-4	415

FTIR spectra of the compounds were obtained. Two peaks were monitored as an indication of metal coordination. Two peaks are associated with the C=N (~1620 cm^{-1}) and N-O (~980 cm^{-1}) bonds, both of which should remain after metallation. For compound **D-3**, the C=N peak shifted -20 cm^{-1} and the N-O peaks shifted +38 cm^{-1}, see Table 10. An FTIR spectra of compound **D-3** and literature assignments for compounds **D1** and **D2** compared to their corresponding ligands can be found in Appendix B.

Table 10: The monitored C=N and N-O peaks for each spectra and reference spectra. The shift column denotes the direction and magnitude of the shift between the ligand and complex.

Complex	**C=N (cm^{-1})**	**Shift (cm^{-1})**	**N-O (cm^{-1})**	**Shift (cm^{-1})**
dmg (lit.)[54]	1620		975	
D-1 (lit)[55]	1619	-1	1009	+34
B-3	1660		912	
D-3	1640	-20	950	+38

The next method of characterization was solution electrochemistry. The reduction potentials **D-3** were analyzed in dichloromethane by cyclic voltammetry. All referenced cyclic voltammograms are in Appendix D. Ferrocene was used as an internal standard in order to calibrate the reference potential in the cyclic voltammograms. For **D-3**, the reduction potential for $Co^{3+/2+}$ and $Co^{2+/1+}$ was found to be -0.242 V vs SCE and -1.56 V vs SCE in dichloromethane, respectively. Literature values for reduction potentials of $Co^{2+/1+}$ in

compounds **D-1** and **D-2** were reported as -0.43 V vs SCE in water,[29] and -0.28 V vs SCE in acetonitrile,[30] respectively, see Table 11.

Table 11: Reduction potential results for compounds **D-1**, **D-2**, and **D-3**.

	$Co^{2+/1+}$ (V vs SCE)		**$Co^{3+/2+}$ (V vs SCE)**
	Experimental	**Literature**	**Experimental**
D-1	-	-0.43[29]	-
D-2	-	-0.28[30]	-
D-3	-1.56[13]	-	-0.126[13]

In characterizing the catalytic activity of the cobaloximes, acid was added to the non-aqueous solution. In the titrations of **D-3** in acetonitrile solution, tosylic acid (pK_a = 8.0) and trifluoroacetic acid (pK_a = 12.7) were used, see Appendix D.[56] As titration proceeded, a catalytic wave developed following the reduction from the cobalt(II) to the cobalt(I) state. Values were obtained by Katarina Hauser.[13]

MALDI-MS was used to finalize characterization of compound **D-3**. MALDI-MS with a t-BPPM-Matrix predicted 975.5 m/z for compound **D-3**, and the observed value was 971.9 m/z.

Discussion

Characterization of Compounds A1-A3

Although many attempts to synthesize compounds **A-1**, **A-2**, and **A-3** were made, no evidence was found to indicate successful synthesis. After pursuing this route of synthesis for several months, it was decided to pursue a new set of compounds.

Characterization of Compounds B1-B5

The synthesis of compound **B-1** was carried out entirely by Drs. Wheeler and Hambourger, due to its hazardous nature. Even though no experimental data of ^{1}H NMR, ^{13}C NMR, or FTIR had been reported prior to this experiment, the presence of only one peak on the ^{13}C NMR, one peak in the ^{1}H NMR, and three distinct stretches in the FTIR indicated the presence and purity of the product; the one peak on the ^{13}C NMR was similar to the singular peak expected in spectral prediction software.

Although evidence was never found indicating the successful synthesis of compound **B-2**, significant evidence was present indicating the formation of compounds **B-3**, **B-4**, and **B-5**. ^{1}H NMR and ^{13}C NMR were taken immediately after compounds were recovered. Compound **B-3** was compared with the literature values confirming the presence of the expected six peaks, see Table 1.[48] These six peaks are associated with the N-O*H*, N-*H*, and various alkyl, C-*H*, protons peaks found in the compound. Integration of each of the peaks confirmed the expected number of protons corresponding with each peak. For compounds **B-4** and **B-5** the five and six expected peaks were observed, respectively, see Table 1.

Compound **B-4** was expected to have similar peaks to **B-3**, but without the N-*H* peak due to the absence of that hydrogen due to a secondary amine side-chain as opposed to the primary amine side chains in compounds **B-3** and **B-5**. The presence of five unique hydrogen peaks, with expected integration, position, and splitting pattern indicated clean **B-4** product.

Compounds **B-5** was expected to have five unique proton peaks, with four unique peaks associated with the cyclohexyl group. However, **B-5** showed evidence of nine unique proton peaks. Integration of the nine peaks provided the expected number of protons at the expected positions and splitting patterns, see Table 1, with no other peaks present in the spectra other than reference solvent peaks indicated that the compound was pure. It is thought that the presence of multiple alkyl proton peaks is due to the difference in orientation in the two cyclohexyl groups, resulting in slightly offset peaks for these protons in the ^{1}H-NMR.

Compounds **B-3**, **B-4**, and **B-5** were expected to have seven, five, and four unique carbon peaks, respectively. Each of the compounds has a carbon peak associated with the *C*-NOH bond. Compound **B-3** has hexyl chain groups, with six distinct carbons, and experimental data confirmed presence of seven distinct peaks in total. Compound **B-4** has dibutyl groups, with four distinct carbons, and experimental data confirmed presence of five distinct peaks in total. Compound **B-5** has cyclohexyl groups, with a predicted four distinct carbons, but experimental data confirmed presence of six distinct carbons in total, see Table 2. This is thought to be due to the fact that the orientation of the cyclohexyl groups causes a slight shift in the carbon peaks that would otherwise be the same.

Finally, FTIR was used to confirm functional groups in compounds **B-1** and **B-3** against reference spectra,[48] and used qualitatively to measure purity. Five stretches were expected for

all the compounds: N-H, O-H, CH_2, C=N, and N-O stretches. Each of the compounds showed only those five stretches, all of which are in the expected range for each stretch, see Table 3.

Characterization of Compounds C1-C5

The initial successful synthesis of compound **C-1** prompted the main focus of the last few semesters of work on this project: to prepare a series of aryl amidoxime derivatives and their corresponding cobaloximes. Although many attempts to synthesize compounds **C-2**, **C-4**, and **C-5** were made, no evidence was ever found to indicate a successful synthesis. Compound **C-3** was synthesized once, but attempts to replicate this synthesis have not been successful.

In characterizing **C-1** and **C-3**, ^{1}H NMR and ^{13}C NMR were initially used. Compound **C-1** had been synthesized and reported previously, so reference NMR data were primarily used to verify purity and identity of the compound.[52] The structure of **C-1** allowed for the prediction of five unique proton shifts in the ^{1}H NMR spectrum: N-O*H*, N-*H*, and three aryl hydrogens. Experimental results showed evidence of five different peaks alone, see Table 4, each corresponding to the correct shift associated with the type of bond. Integration of the peaks verified the presence of the correct number of protons expected for the molecule, each of which exhibited the proper splitting pattern. Furthermore, it was expected that **C-1** would show evidence of five different carbon peaks: *C*-NOH and four aryl carbons. Experimental data showed evidence of five carbon peaks. Both the ^{1}H NMR and ^{13}C NMR were compared to reference data, and the peak shifts were almost identical, see Tables 4 and 5.[52]

For compound **C-3**, no reference data has been reported to compare results. Instead, the peak shifts were predicted through an understanding of theory and compared against shifts

in **C-1**. The difference between **C-1** and **C-3** is the presence of a methoxy group on **C-3**. This addition adds two extra protons overall, which were all present according to integration data. The presence of each of the notable peaks, N-O*H*, N-*H*, and aryl hydrogens, were all accounted for, see Table 4. Furthermore, it was expected that **C-3** would show evidence of six different carbon peaks: *C*-NOH, O-*C*H3, and the four aryl carbons. Experimental data showed evidence of six carbon peaks, see Table 5. As there was a lack of evidence of any impurities in the product, it was concluded that the product had been successfully made.

Finally, FTIR was used to confirm the identity and purity of **C-3** against a reference spectrum, and used to identify compounds **C-1** by comparing stretches against **C-3**, see Table 6. Five stretches were expected for compound **C-1**: N-H, O-H, CH_2, C=N, and N-O stretches. Each of the compounds showed only those five stretches, each in the expected range for each stretch. Furthermore, **C-3** showed more CH_2 stretches than **C-1**, which was expected due to the presence of methoxy group in **C-3**.

Characterization of Compounds D1-D4

Magnetic susceptibility data showed that the compound **D-4** had one unpaired electron, demonstrating that this complex had a paramagnetic cobalt(II), d^7, low-spin center. The number of unpaired electrons via magnetic susceptibility was unable to be determined for **D-3**, because only a few milligrams of solid were purified from the mostly oily product. Instead, a ^{1}H NMR spectrum was taken of the complex and showed evidence of diamagnetic properties, unlike compound **D-4**. Paramagnetic compounds have an unpaired electron which has a magnetic moment. Paramagnetic metal centers broaden the NMR peaks, and having sharp peaks in the NMR spectra was taken as evidence of a diamagnetic cobalt(III), d^6, low spin

center. After further purification of the compounds, ^{1}H NMR and ^{13}C NMR spectra were taken of **D-3**, see Tables 7 and 8, and again showed diamagnetic properties, confirming that the compound was present instead of the suspected unreacted ligand, **B-3**.

When the ^{1}H NMR spectra of **B-3** and **D-3** were compared, see Table 7, the OH group in the **B-3** was not present in spectrum for **D-3**; this is expected due to the breaking of the OH bond that is replaced with the BF_2 capping group during synthesis of **D-3**. Other than this one difference, the spectra are very similar. When the ^{13}C NMR spectra of **B-3** and **D-3** were compared, see Table 8, there were only minor differences in chemical shifts, most likely due to the small change in chemical environment between the ligand alone and in the complex. The fact that an NMR spectra was obtained for **D-3** suggests that the complex is not paramagnetic cobalt(II), but exists as diamagnetic, low-spin cobalt(III). This conclusion was also backed by cobaloxime studies comparing H-capped and BF_2 capped **D-1** derivatives.[29] In the BF_2 capped **D-1**, the cobalt(II) center is not reducing enough to react with O_2 under ambient conditions. In **D-3**, however, the cobalt(II) center is so electron rich that it spontaneously reduces O_2 in the reaction flask and is isolated as cobalt(III). The H-capped **D-1** is also isolated as cobalt(III) for the same reason.[29]

The next characterization was UV-visible spectroscopy. The UV-visible band, which indicates the change in energy from the highest occupied molecular orbital (HOMO) to the lowest occupied molecular orbital (LUMO), occurs in these cobaloximes through a metal ligand charge transfer (MLCT) process, in which the electrons in a d-orbital on a metal are promoted to a vacant π^* ligand orbital. In the compounds **D-1**, **D-2**, and **D-4**, each of which are thought to be in cobalt(II) state, an increase in λ_{max} is seen to occur whenever the electron density of the cobalt ion is decreased. In **D-2**, the phenyl side chains on the cobaloxime are

electron withdrawing, and cause a shift in λ_{max} to a longer wavelength than in **D-1**. This is thought to occur due to the π^* orbital from the phenyl ring having a lower energy than the π^* orbital available in the **D-1**. In **D-4**, the aniline side chains are electron donating, and cause a shift in λ_{max} to shorter in wavelength than in **D-1**. This is thought to occur due to the π^* orbital from the phenyl ring having a higher energy than the π^* orbital available in the **D-1**. Compound **D-3** is thought to be in the cobalt(III) state, and has a λ_{max} valu of wavelength much longer than any of the other compounds, see Table 9.

The next characterization was FTIR spectroscopy. In the FTIR spectra, it is expected that the majority of peaks are not shifted upon complex formation. However, the peak associated with the OH bond is expected to be absent in the metal complex since it is broken when the complex forms so that the BF_2 group can attach. Furthermore, bonds involving the imine nitrogen atoms will be affected due to coordination of the metal directly to these atoms. Therefore, the absence of OH peaks and shifting of C=N and N-O stretches were used to verify formation of cobaloxime. Compounds **D-1**, **D-2**, and **D-3** all experienced similar shifts in magnitude and direction. The shift in N-O peaks indicates a shift to higher frequency corresponding to the new bonding environment. Since the N-O stretch is affected by the O-H stretch, and the proton is being replaced by a boron atom during the bridging by BF_2, the more rigid O-B bond causes the N-O bond to have less freedom, and become more rigid itself and therefore, high frequency stretching. The shift in the C=N stretch to a lower stretching frequency indicates that the double bond is weakened, caused by the nitrogen atom being pulled farther away by the cobalt center. These data help to confirm that the final compounds are different than the corresponding ligand starting materials, see Table 10. Furthermore, a noticeable broadening of peaks associated with where BF_2 peaks should appear is also shown.[55]

The final characterization was solution electrochemistry of the cobaloximes. The cobalt centers are thought to be catalytically active for the reduction of protons to H_2. The ligands are used to tune the potential at which the reduction of cobalt(II) to cobalt(I), or cobalt (III) to cobalt (II) occur. Compared to the electron withdrawing phenyl substituent on **D-2**, the electron donating N-alkyl substituent on **D-3** allowed cobalt (II) to form at a lower potential than in either **D-1** or **D-2**, see Table 11. The catalytic activity of **D-3** was confirmed via titration with trifluoroacetic acid. As the cobalt(III) to cobalt(II) transition was observed, the following heterolytic mechanism, shown in Figure 9, could be a possibility. Full experimental detail and results can be found in reference 13.

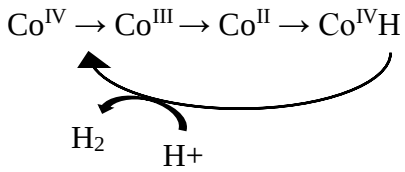

Figure 9: Possible mechanism for **D-3** if the resting state for the complex is cobalt(III).

After analysis of the N-alkyl glyoxime showed that increased electron density on the central cobalt ion shifted the reduction potential of the cobalt(III) to cobalt(II) transition, it became clear that fine-tuning of the ligand was the next step in attempting neutral pH water electrolysis through a cobaloxime. To this end, synthetic efforts were refocused from N-alkyl glyoximes to N-aryl glyoximes. The synthesis of new substituted N-aryl cobaloximes will likely confirm the hypothesis that electron donating substituents allow catalytic turnover in a less acidic pH environment. However, there are several complications with the syntheses that must be overcome in order to reach this goal. Repeated attempts at synthesis of compounds

C-2, **C-4**, and **C-5** in different solvents and at different temperatures have failed to show any reaction between the dichloroglyoxime and the aniline derivatives. Failure to successfully create these glyoximes prohibits the synthesis of their corresponding cobaloximes. Furthermore, synthesis of **D-3** and **D-4** were very complicated due to the formation of oily compounds instead of the powdery solids acquired for compounds **D-1** and **D-2**. One of the potential reasons that these syntheses either fail to react or decompose is due to the high temperatures required, which perhaps are resulting in the formation of polyaniline chains between the ligands. If these compounds can be synthesized successfully, electrochemical data will provide more insight to the electronic properties of the cobalt center; specifically, it will be interesting to see if the cobalt(III) to cobalt(II) transition is still observed in the electron donating *p*-substitute aniline cobaloxime derivatives, and if this transition occurs at a lower or higher reduction potential.

If these derivatives can in fact permit catalytic turnover under a neutral pH environment, then they can potentially be utilized in scalable technologies for the production of molecular hydrogen. Increasing the amount of molecular hydrogen available for use in the real world will help to meet the growing energy demands of the populace, while mitigating the side-effects of non-renewable energy on planet Earth.

Future Work

While working on this project, I was only able to successfully synthesize and characterize **B-3**, **B-4**, **B-5**, **C-1**, **C-3**, **D-3**, and **D-4**. However, many of the *p*-substituted aniline cobaloximes were unable to be made. Future efforts by those in the lab continuing in this project will hopefully garner more success in this endeavor. If so, many of these ligands would be new glyoximes and all of the analogous cobaloximes would be new compounds. These ligands would be characterized by NMR, IR, UV-visible, and MS, and the resultant metallated complexes would be characterized by IR, UV-visible, MS, and magnetic susceptibility. Heteronuclear NMR would also be used in analysis of the cobaloximes, but a decrease in the resolution would be expected due to the paramagnetic cobalt(II) ion. Furthermore, it would be expected that future members of my lab or Dr. Hambourger's lab would evaluate the hydrogen catalytic properties of the cobaloximes via electrochemical analysis.

Conclusions

Six glyoximes were synthesized and characterized by CHN analysis, ^{1}H NMR spectroscopy, ^{13}C NMR spectroscopy, and FTIR spectroscopy. Four cobaloximes were synthesized and characterized by CHN analysis, magnetic susceptibility, ^{1}H NMR spectroscopy, ^{13}C NMR spectroscopy, UV-visible spectroscopy, FTIR spectroscopy, and CV. The three known glyoximes, **B-1**, **B-3**, and **C-1**, and two known cobaloximes, **D-1** and **D-2**, showed results that were similar to published materials. The novel glyoximes **B-4**, **B-5**, and **C-3** each showed similar results to the known glyoximes, suggesting formation of the compounds. The novel cobaloximes **D-3** and **D-4** showed similar results to the known cobaloximes, which suggests the complexes were formed. One noticeable difference between **D-3** and the **D-1** and **D-2** compounds was that it was thought to exist as cobalt(III) instead of cobalt(II). Acid titration with trifluoroacetic acid and tosylic acid demonstrate cobaloximes catalytic activity for hydrogen production. Additional work will be required to carry out syntheses of compounds **C-2**, **C-4**, and **C-5**, and their corresponding cobaloximes.

Financial Support

Funding for this project has been provided by the Appalachian State University Office of Student Research in the form of numerous research grants, numerous travel grants, and numerous research assistantships, the College of Arts and Sciences, the A.R. Smith Department of Chemistry, the Sigma Xi Grants-In-Aid-of-Research Grant, the George T. Barthalmus Undergraduate Research Grant, and the Barry M. Goldwater Scholarship and Excellence in Education program.

References

(1) U.S. Department of Energy; Annual Energy Outlook, **2013**, US Energy Information Administration: Washington, DC, 2013.

(2) Lewis, N. S.; Nocera, D. G. *Proc. Natl. Acad. Sci. U. S. A.* **2006**, *103*, 15729.

(3) Sorensen *Renewable Energy, Third Edition*; Academic, **2004**.

(4) Hambourger, M.; Moore, G. F.; Kramer, D. M.; Gust, D.; Moore, A. L.; Moore, T. A. *Chem. Soc. Rev.* **2009**, *38*, 25.

(5) IPCC, 2014: *Climate Change 2014: Impacts, Adaptation, and Vulnerability. Part A.*; Field, C.B., et al. (eds.)]. New York, NY, USA. 2014, 1132 pp.

(6) Song, W.; Chen, Z.; Brennaman, M. K.; Concepcion, J. J.; Patrocinio, A. O. T.; Iha, N. Y. M.; Meyer, T. J. *Pure Appl. Chem.* **2011**, *83*, 749.

(7) Ming, Q; Healey, T; Allen, Lloyd, Irving, P. *Catal. Today*. **2002**, *77*, 51.

(8) Navarro, R. M.; Pena, M. A.; Fierro, J. L. G. *Chem. Rev. (Washington, DC, U. S.)* **2007**, *107*, 3952.

(9) Lessing, P. A. *J. Mater. Sci.* **2007**, *42*, 3477.

(10) Dempsey, J. L.; Brunschwig, B. S.; Winkler, J. R.; Gray, H. B. *Acc. Chem. Res.* **2009**, *42*, 1995.

(11) Esswein, A. J.; Nocera, D. G. *Chem. Rev. (Washington, DC, U. S.)* **2007**, *107*, 4022.

(12) Gray, H. B. *Nat. Chem.* **2009**, *1*, 7.

(13) Hauser, K. *Synthesis, Surface Immobilization, and Electrochemical Characterization of Cobalt bis(glyoxime) Hydrogen Catalysts*. **2014** (Undergraduate Thesis).

(14) Campbell *Biology, Tenth Edition*. **2014**, pp. 205.

(15) Bard, A. J.; Fox, M. A. *Acc. Chem. Res.* **1995**, *28*, 141.

(16) Darensbourg, M. Y.; et al. *Proc. Natl. Acad. Sci., USA.* **2003**, *100*, 3683.

(17) Volbeda, A.; Fontecilla-Camps, J. C. *Coord. Chem. Rev.* **2005**, *249*, 1609.

(18) Jones, A. K.; Sillery, E; Albracht, S. P. J.; Armstrong, F.S. *Chem. Commun*. **2002**, *8*, 866.

(19) Hambourger, M.; et al. *J. Am. Chem. Soc.* **2008**, *130*, 2015.

(20) Gloaguen, F.; Rauchfuss, T. B. *Chem. Soc. Rev.* **2009**, *38*, 100.

(21) Le Goff, A.; et al. *Int. J. Hydrogen. Energ.* **2010**, *35*, 10790.

(22) Wilson, A. D.; et al. *J. Am. Chem. Soc.* **2006**, *128*, 358.

(23) Kellett, R. M.; Spiro, T. G. *Inorg. Chem.* **1985**, *24*, 2378.

(24) Collin, J. P.; et al. *Inorg. Chem.* **1988**, *27*, 1986.

(25) Artero, V.; Fontecave, M. *Coord. Chem. Rev.* **2005**, *249*, 1518.

(26) Bakac, A.; et al. *Inorg. Chem.* **1986**, *25*, 4108.

(27) Chao, T. H.; Espenson, J. H. *J. Am. Chem. Soc.* **1978**, *100*, 129.

(28) Schrauzer, G. N. *Acc. Chem. Res.* **1968**, *1*, 97.

(29) Connolly, P.; Espenson, J. H. *Inorg. Chem.* **1986**, *25*, 2684.

(30) Hu, X.; Cossairt, B. M.; Brunschwig, B. S.; Lewis, N. S.; Peters, J. C. *Chem. Commun. (Cambridge, U. K.)* **2005**, 4723.

(31) Razavet, M.; Artero, V.; Fontecave, M. *Inorg. Chem.* **2005**, *44*, 4786.

(32) Eckenhoff, W. T.; McNamara, W. R.; Du, P.; Eisenberg, R. *Biochim. Biophys. Acta, Bioenerg.* **2013**, *1827*, 958.

(33) Artero, V.; Chavarot-Kerlidou, M.; Fontecave, M. *Angew. Chem., Int. Ed.* **2011**, *50*, 7238.

(34) McCormick, T. M.; Han, Z.; Weinberg, D. J.; Brennessel, W. W.; Holland, P. L.; Eisenberg, R. *Inorg. Chem.* **2011**, *50*, 10660.

(35) Solis, B. H.; Hammes-Schiffer, S. *Inorg. Chem.* **2011**, *50*, 11252.

(36) Dempsey, J. L.; Winkler, J. R.; Gray, H. B. *J. Am. Chem. Soc.* **2010**, *132*, 16774.

(37) Baffert, C.; Artero, V.; Fontecave, M. *Inorg. Chem.* **2007**, *46*, 1817.

(38) Dempsey, J. L.; Winkler, J. R.; Gray, H. B. *J. Am. Chem. Soc.* **2010**, *132*, 1060.

(39) Du, P.; Schneider, J.; Luo, G.; Brennessel, W. W.; Eisenberg, R. *Inorg. Chem.* **2009**, *48*, 4952.

(40) McCormick, T. M.; Calitree, B. D.; Orchard, A.; Kraut, N. D.; Bright, F. V.; Detty, M. R.; Eisenberg, R. *J. Am. Chem. Soc.* **2010**, *132*, 15480.

(41) Felton, G. A. N.; Glass, R. S.; Lichtenberger, D. L.; Evans, D. H. *Inorg. Chem.* **2006**, *45*, 9181.

(42) Veldkamp, B. S.; Han, W.-S.; Dyar, S. M.; Eaton, S. W.; Ratner, M. A.; Wasielewski, M. R. *Energy Environ. Sci.* **2013**, *6*, 1917.

(43) Berben, L. A.; Peters, J. C. *Chem. Commun. (Cambridge, U. K.)* **2010**, *46*, 398.

(44) Tidwell, T. T; *Angew. Chem. Int. Ed*. **2001**, *40*, 331.

(45) Black, C.B.; Andrioletti, B.; Try, A.C.; Ruiperez, C.; Sessler, J.L. *J. Am. Chem. Soc.* **1999,** *121*, 10438-10439.

(46) Lance, K. A.; Goldsby, K. A.; Busch, D. H. *Inorg. Chem*. **1990**, *29*, 4537.

(47) Kim, D. *U.S. Patent No. US7,604,919,B2*. **2009**.

(48) Gümüş, G.; Ahsen, V.; Lebrun, C.; Luneau, D.; Pécaut, J. *New. J. Chem.* **2004**, *28*, 177.

(49) Schrauzer, G. N.; Windgassen, R. J. *J. Am. Chem. Soc.* **1966**, *88*, 3738.

(50) Tovrog, B. S.; Kitko, D. J.; Drago, R. S. *J. Am. Chem. Soc.* **1976**, *98*, 5144.

(51) Noviandri, I.; Brown, K. N.; Fleming, D. S.; Gulyas, P. T.; Lay, P. A.; Masters, A. F.; Phillips, L. *J. Phys. Chem. B.* **1999**, 103, 6713.

(52) Yuksel, F.; Gürek, A. G.; Drumus, M.; Gürol, I.; Ahsen, V.; Jeanneau, E.; Luneau, D. *Inorg. Chim. Acta.* **2008**, *361*, 2225.

(53) Dempsey, J. L. **2011**. *Hydrogen evolution catalyzed by cobaloximes* (Doctoral dissertation).

(54) Keresztury, G.; Holly, S. *Spectrochim. Acta, Part A* **1977**, *33A*, 29.

(55) Lawson, E. E.; Edwards, H. G. M.; Johnson, A. F. *Spectrochim. Acta, Part A* **1994**, *50A*, 1899.

(56) Izutsu, K. *Acid-Base Dissociation Constants in Dipolar Aprotic Solvents*; Blackwell Scientific Publ., **1990**.

Vita

Corbin Daniel Ester was born in Winston-Salem, North Carolina, United States of America on May 25, 1993 to Geral and Karen Ester. He graduated *Summa Cum Laude* from Appalachian State University with University and Departmental Honors. He has a Bachelor's of Science in Chemistry and minors in Biology and Medical Humanities.

Corbin was a participant in the NSF-REU Program at the University of Kentucky in 2012, the CPRTP MD Anderson Cancer Research Center in 2013, and the NIH SIP at the National Cancer Institute in 2014. He has presented his research at ten conferences including the Southeast Regional Meeting of the ACS and the National ACS Meeting in 2013.

Corbin was a Chancellor Scholarship recipient for the graduating class of 2015, and was further awarded several internal and external grants and awards during his time at Appalachian State University. Among the most prestigious of these are the Sigma Xi Grants-In-Aid-of-Research (GIAR) Grant, the George T. Barthalmus Undergraduate Research Grant, the ACS Carolina-Piedmont Excellence in Scholastic Achievement Award, the Barry M. Goldwater Scholarship, the 2013 Appalachian State University Sigma Xi Outstanding Undergraduate Research Award, and the A.R. Smith Department of Chemistry Outstanding Senior of the Year award.

During his time at Appalachian, Corbin served as President of the Health Professions Club, Peer Advisor in the Health Professions Advising Office, Executive Associate Editor of IMPULSE, and founding Vice-President of Alpha Epsilon Delta Carolina Theta Chapter.

In fall 2015, Corbin will be starting a cancer research training assistantship at the NCI under Dr. Paul S. Meltzer. After this experience, Corbin hopes to apply to MD/PhD programs with the long-term goal of becoming a physician scientist.

Appendices

Appendix A – NMR spectroscopy data

Compound B-1

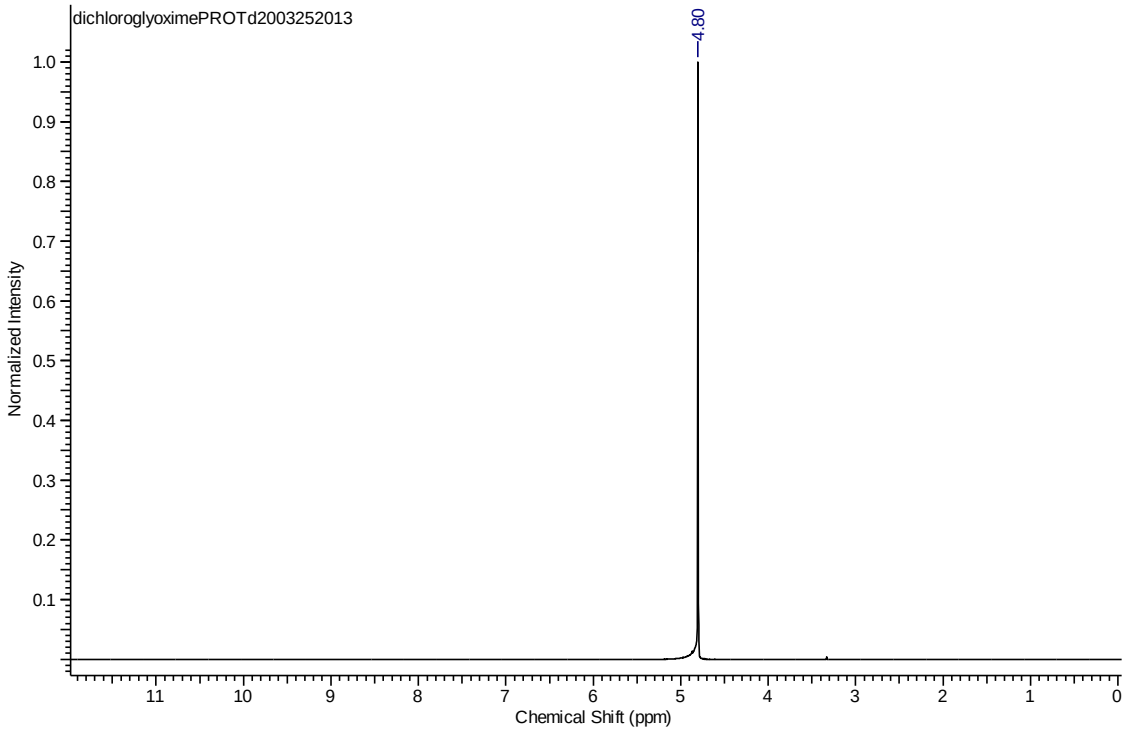

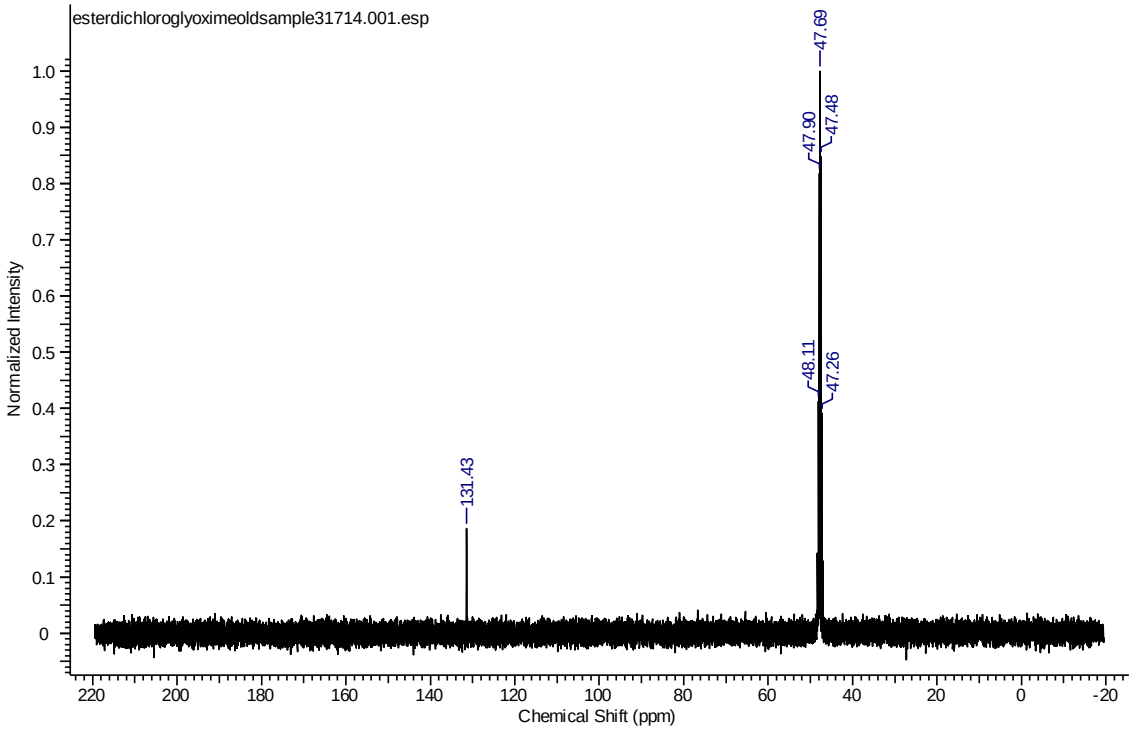

Compound B-3

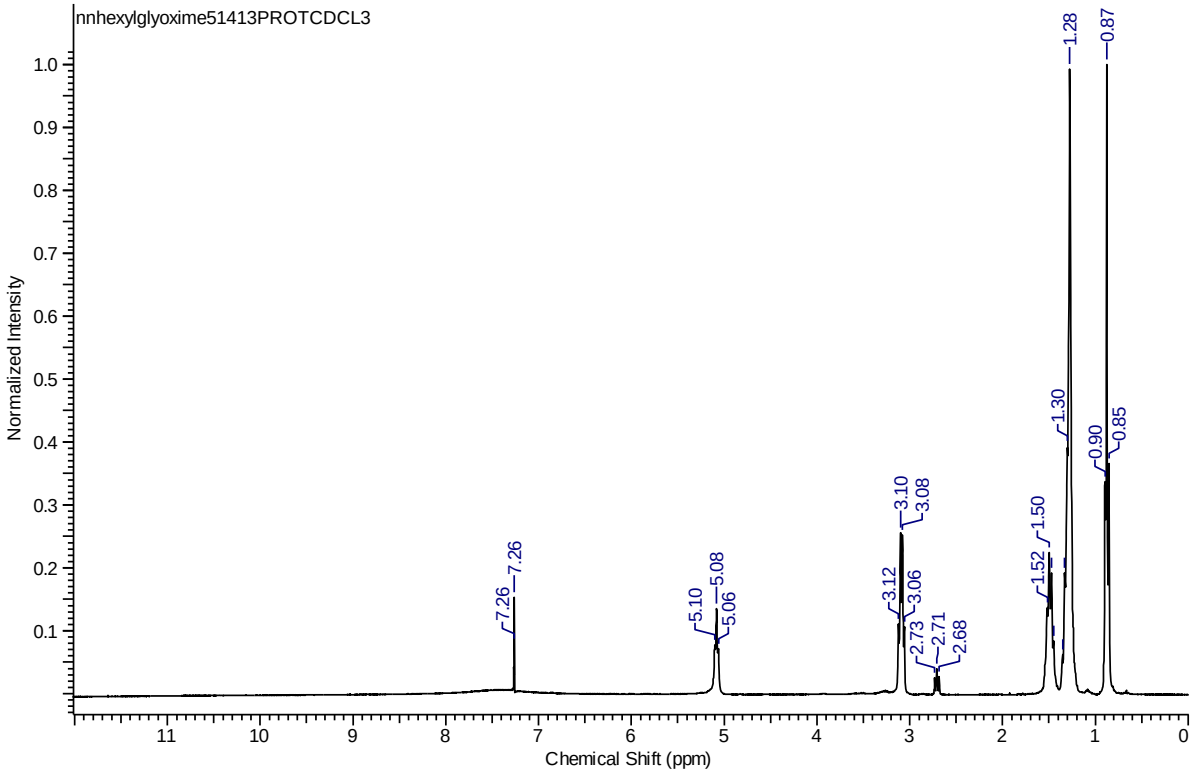
nnhexylglyoxime51413PROTCDCL3
Normalized Intensity
Chemical Shift (ppm)
7.26
7.26
5.10
5.08
5.06
3.12
3.10
3.08
3.06
2.73
2.71
2.68
1.52
1.50
1.30
1.28
0.90
0.87
0.85

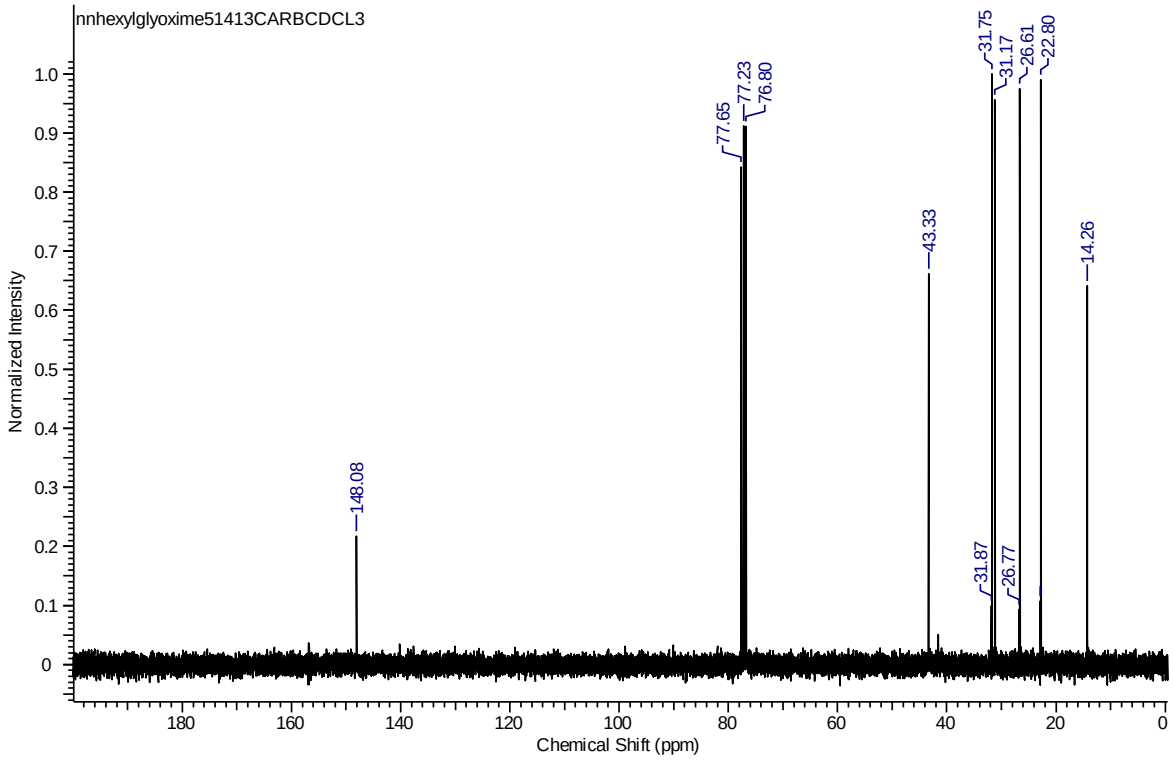
nnhexylglyoxime51413CARBCDCL3
Normalized Intensity
Chemical Shift (ppm)
148.08
77.65
77.23
76.80
43.33
31.87
31.75
31.17
26.77
26.61
22.80
14.26

Compound B-4

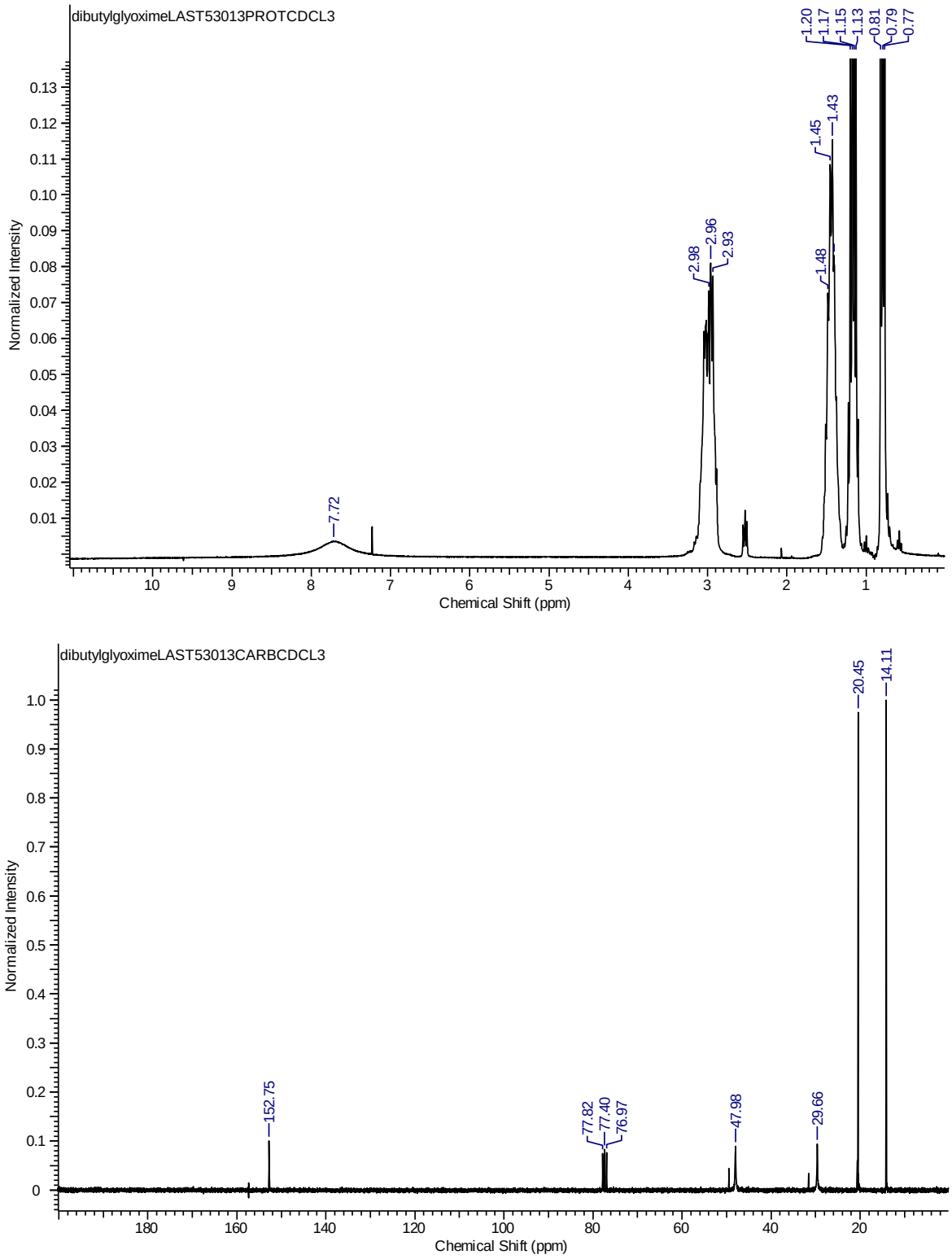
dibutylglyoximeLAST53013PROTCDCL3
Normalized Intensity
Chemical Shift (ppm)
7.72
2.98
2.96
2.93
1.48
1.45
1.43
1.20
1.17
1.15
1.13
0.81
0.79
0.77
dibutylglyoximeLAST53013CARBCDCL3
Normalized Intensity
Chemical Shift (ppm)
152.75
77.82
77.40
76.97
47.98
29.66
20.45
14.11

Compound B-5

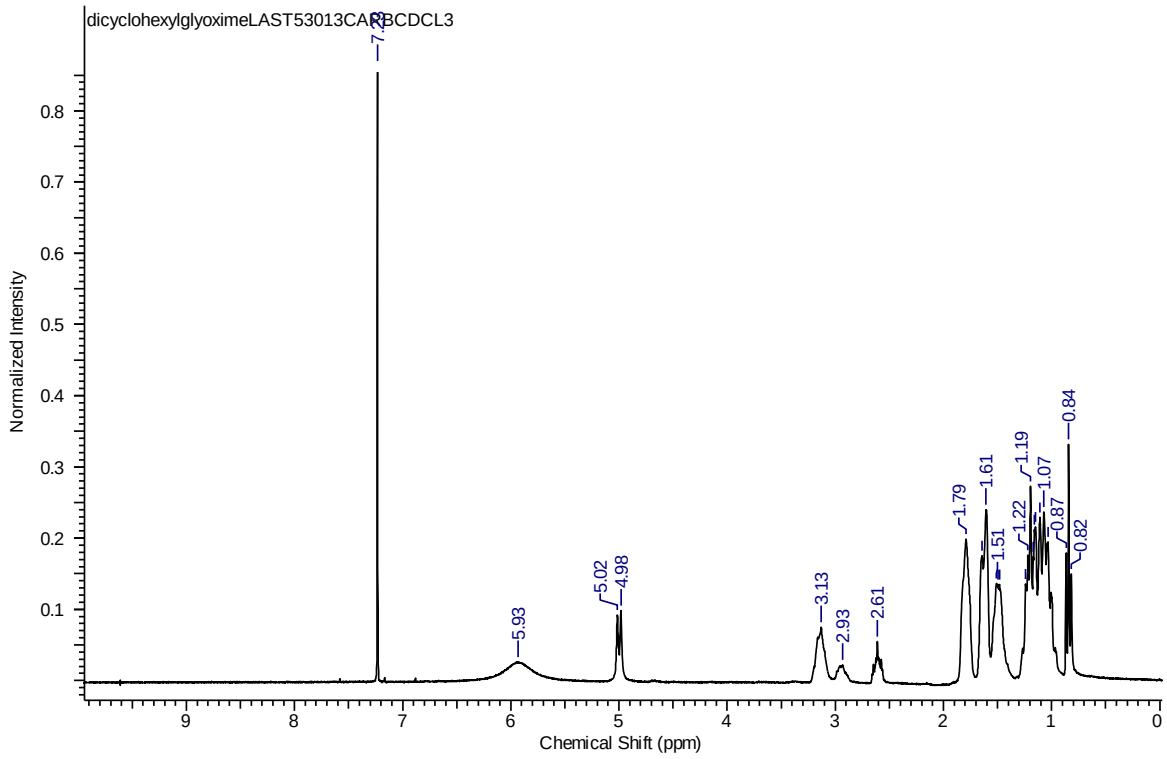
dicyclohexylglyoximeLAST53013CARBCDCL3
Normalized Intensity
Chemical Shift (ppm)
7.26
5.93
5.02
4.98
3.13
2.93
2.61
1.79
1.61
1.51
1.22
1.19
1.07
0.87
0.84
0.82

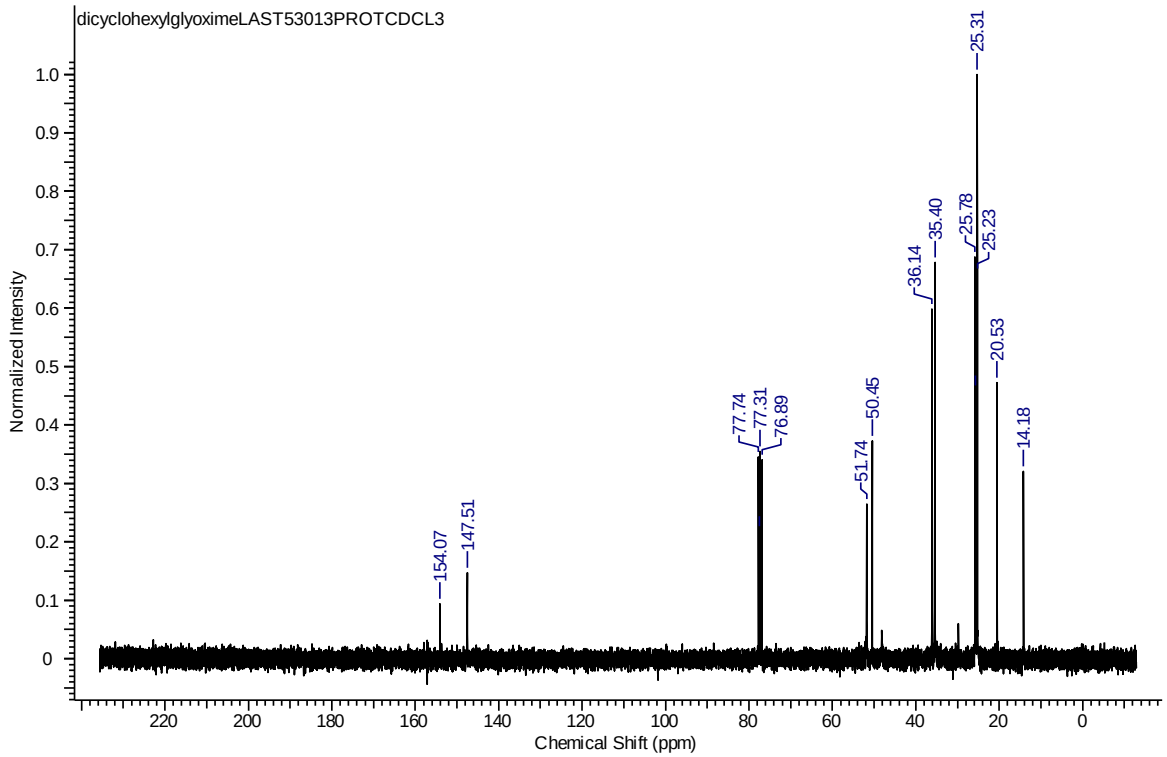
dicyclohexylglyoximeLAST53013PROTCDCL3
Normalized Intensity
Chemical Shift (ppm)
154.07
147.51
77.74
77.31
76.89
51.74
50.45
36.14
35.40
25.78
25.31
25.23
20.53
14.18

Compound C-1

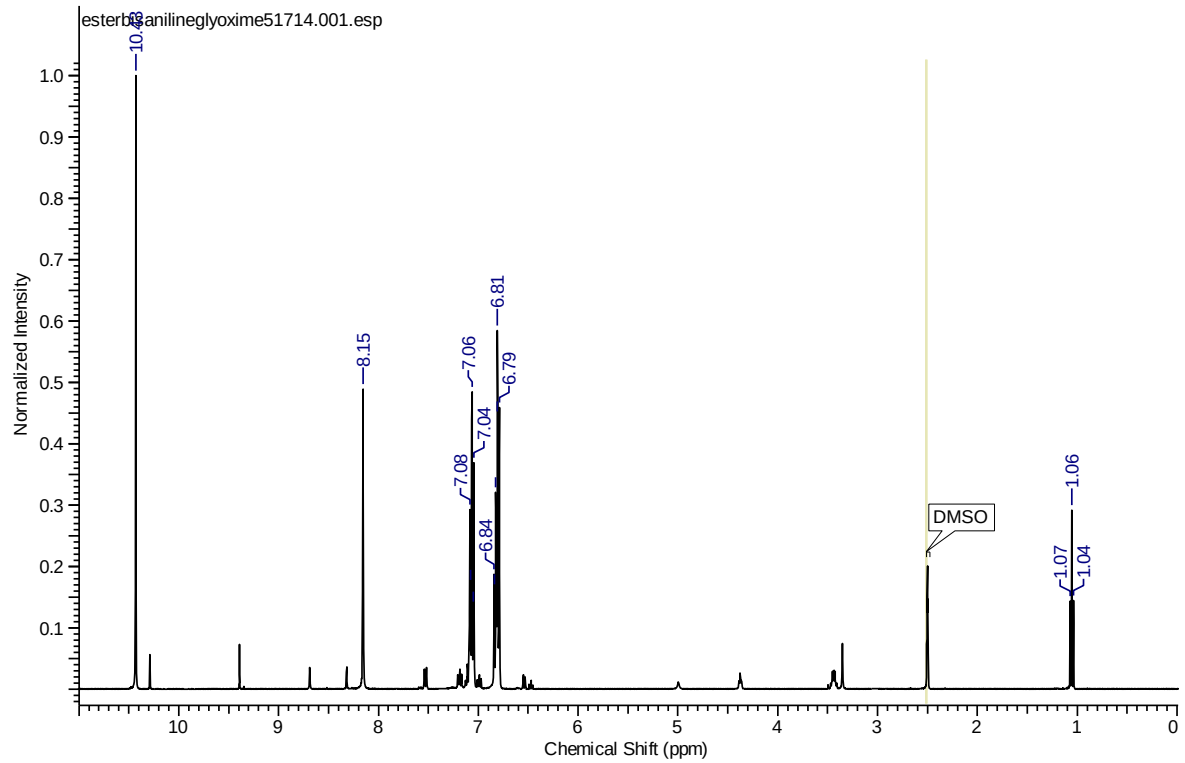
esterbisanilineglyoxime51714.001.esp
Normalized Intensity
Chemical Shift (ppm)
10.43
8.15
7.08
7.06
7.04
6.84
6.81
6.79
DMSO
1.07
1.06
1.04

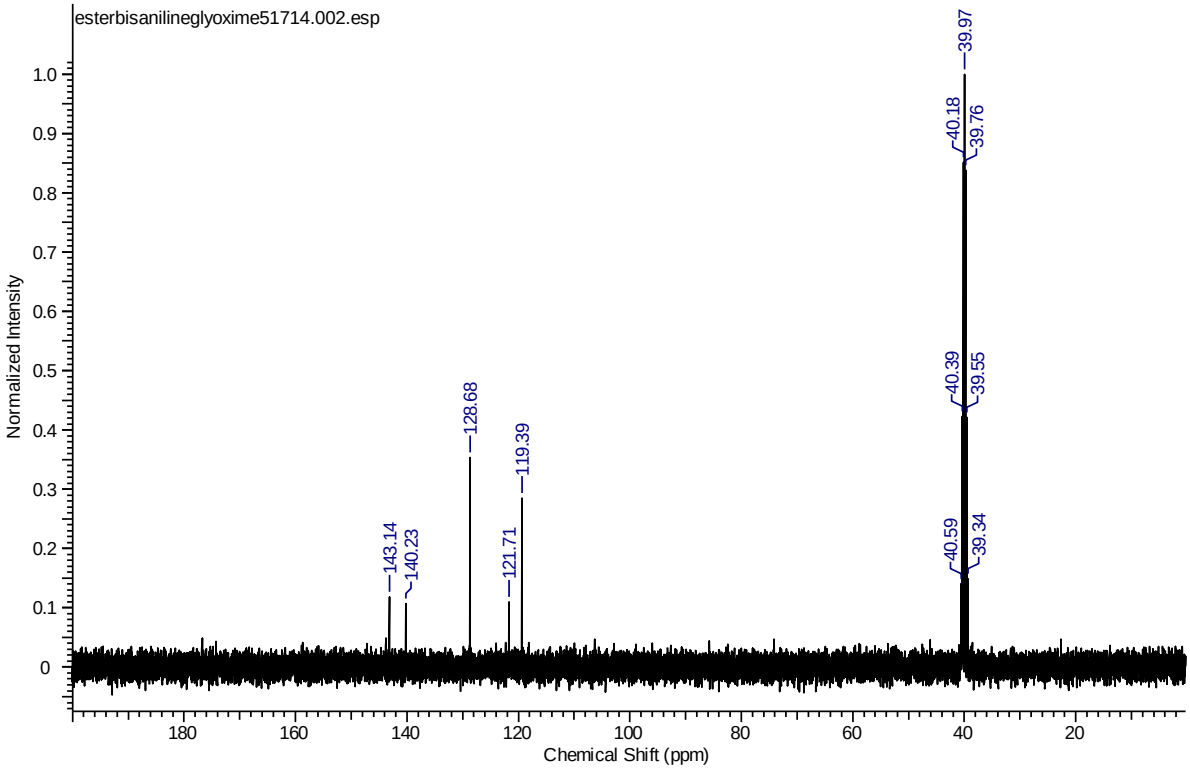
esterbisanilineglyoxime51714.002.esp
Normalized Intensity
Chemical Shift (ppm)
143.14
140.23
128.68
121.71
119.39
40.59
40.39
40.18
39.97
39.76
39.55
39.34

Compound C-3

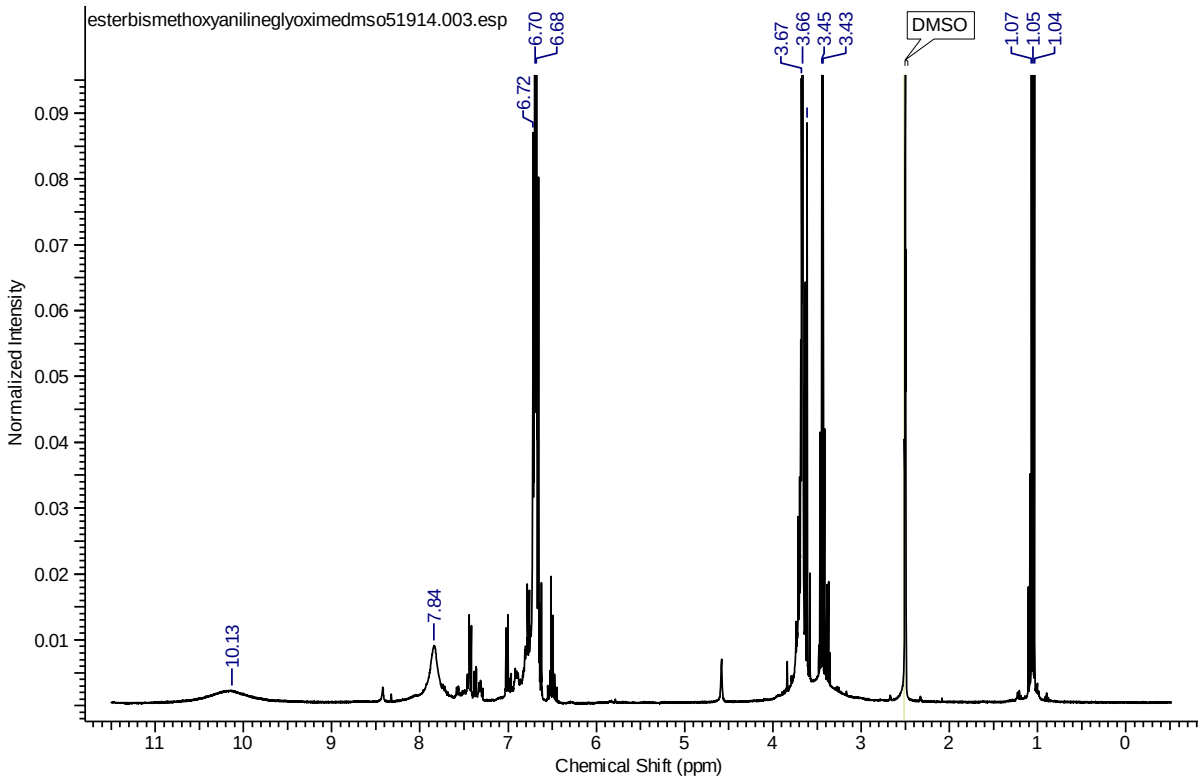
esterbismethoxyanilineglyoximedmso51914.003.esp
6.70
6.68
6.72
3.67
3.66
3.45
3.43
DMSO
1.07
1.05
1.04
10.13
7.84
Normalized Intensity
Chemical Shift (ppm)

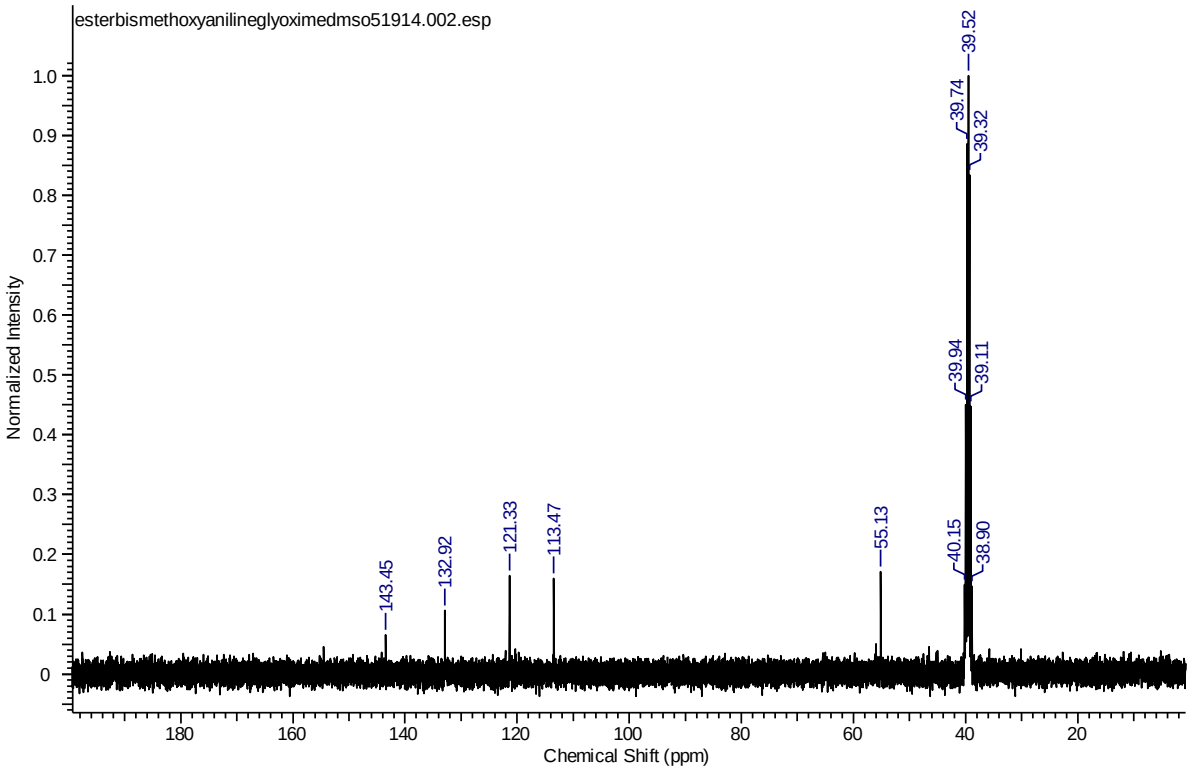
esterbismethoxyanilineglyoximedmso51914.002.esp
39.52
39.74
39.32
39.94
39.11
143.45
132.92
121.33
113.47
55.13
40.15
38.90
Normalized Intensity
Chemical Shift (ppm)

Compound D-3

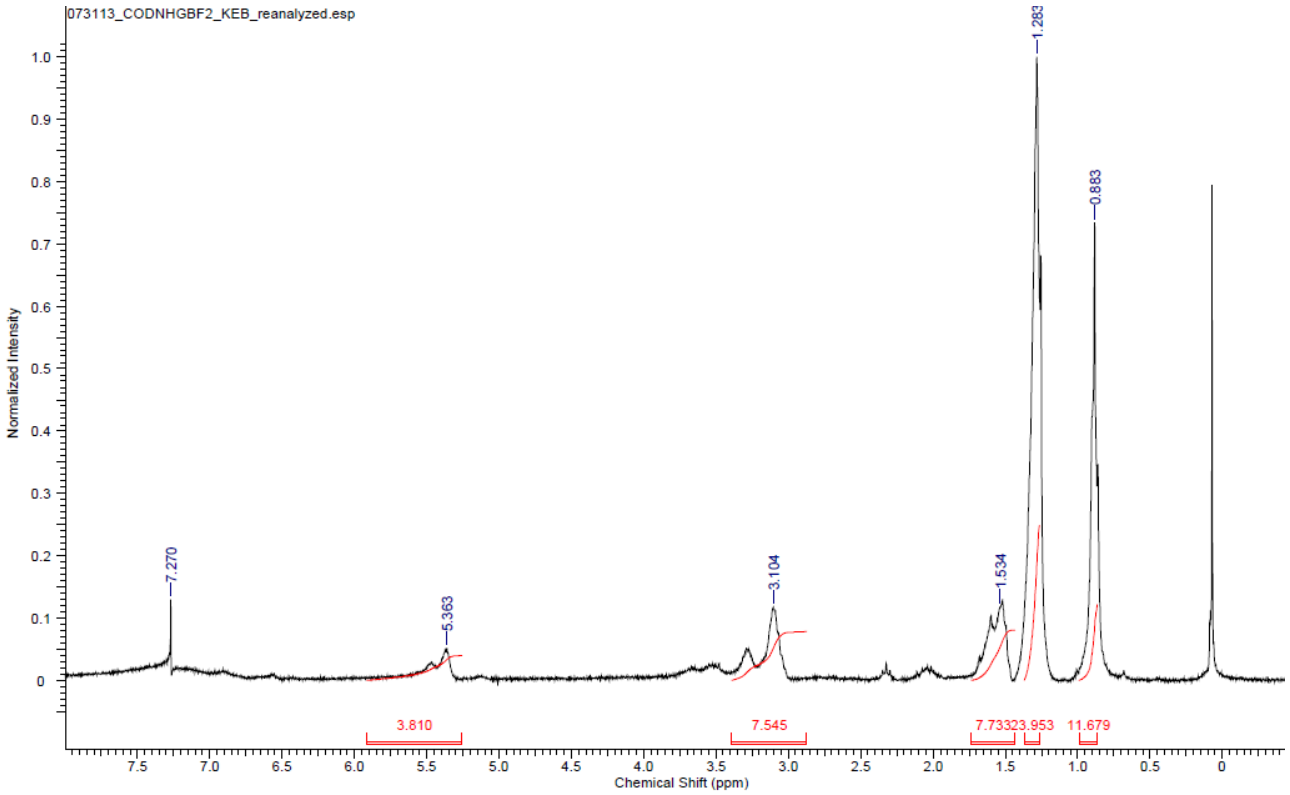
073113_CODNHGBF2_KEB_reanalyzed.esp
Normalized Intensity
Chemical Shift (ppm)
7.270
5.363
3.104
1.534
1.283
0.883
3.810
7.545
7.733
23.953
11.679

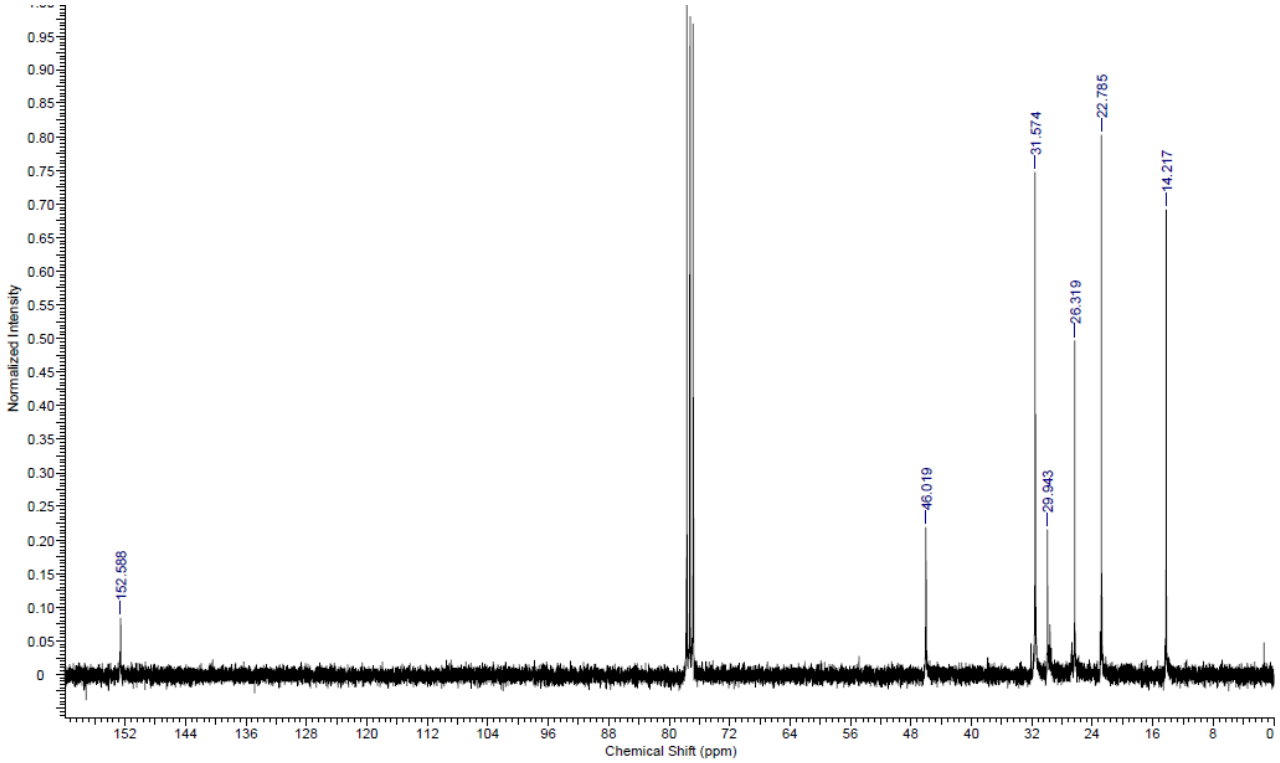
Normalized Intensity
Chemical Shift (ppm)
152.588
46.019
31.574
29.943
26.319
22.785
14.217

Appendix B – FTIR spectroscopy data

Compound B-4

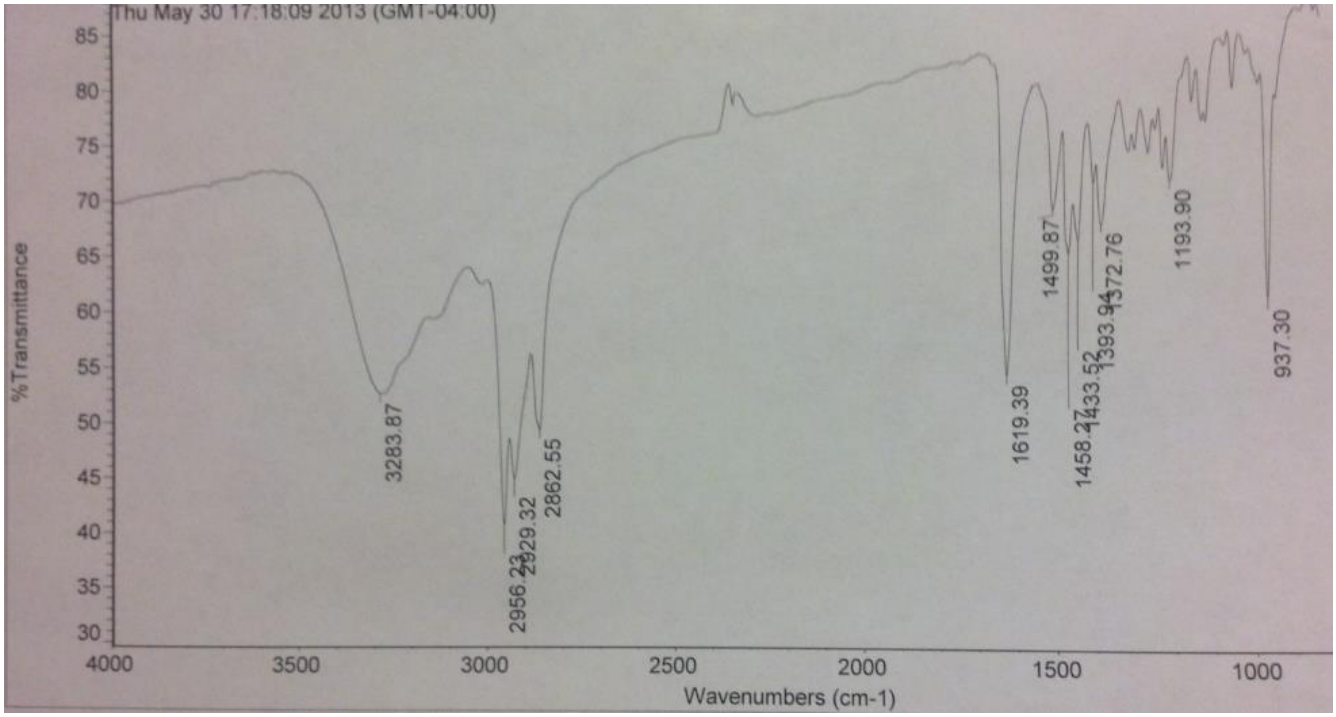

Compound B-5

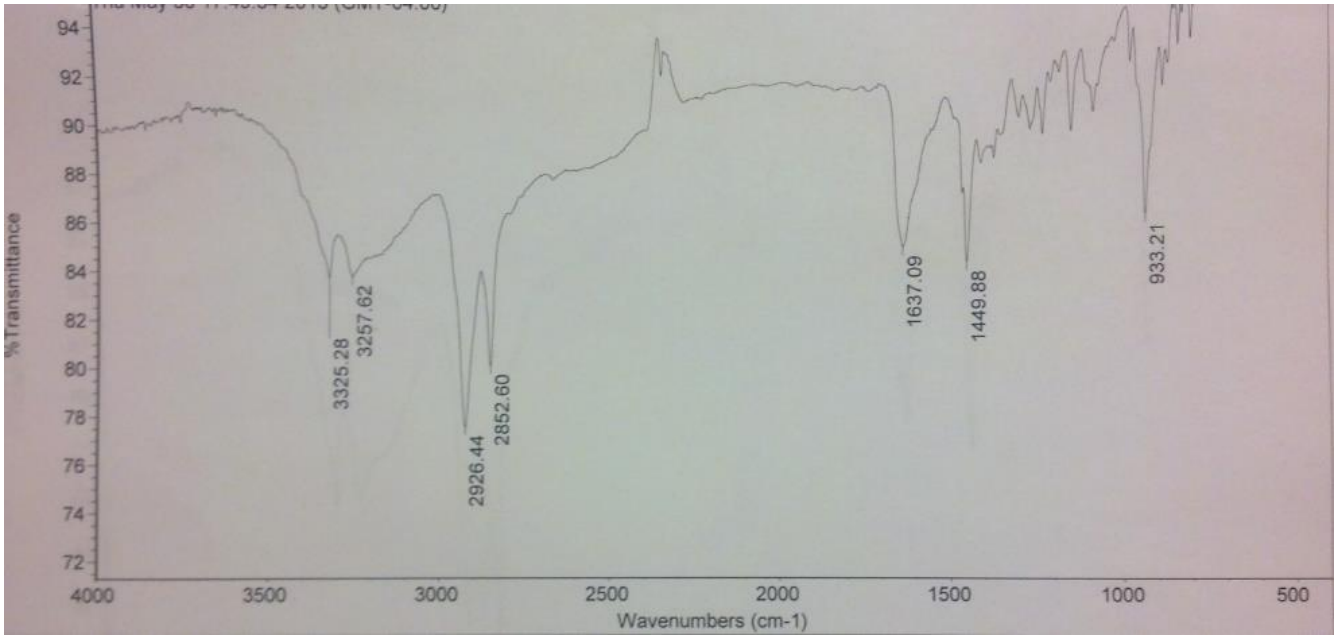

Compound C-1

A

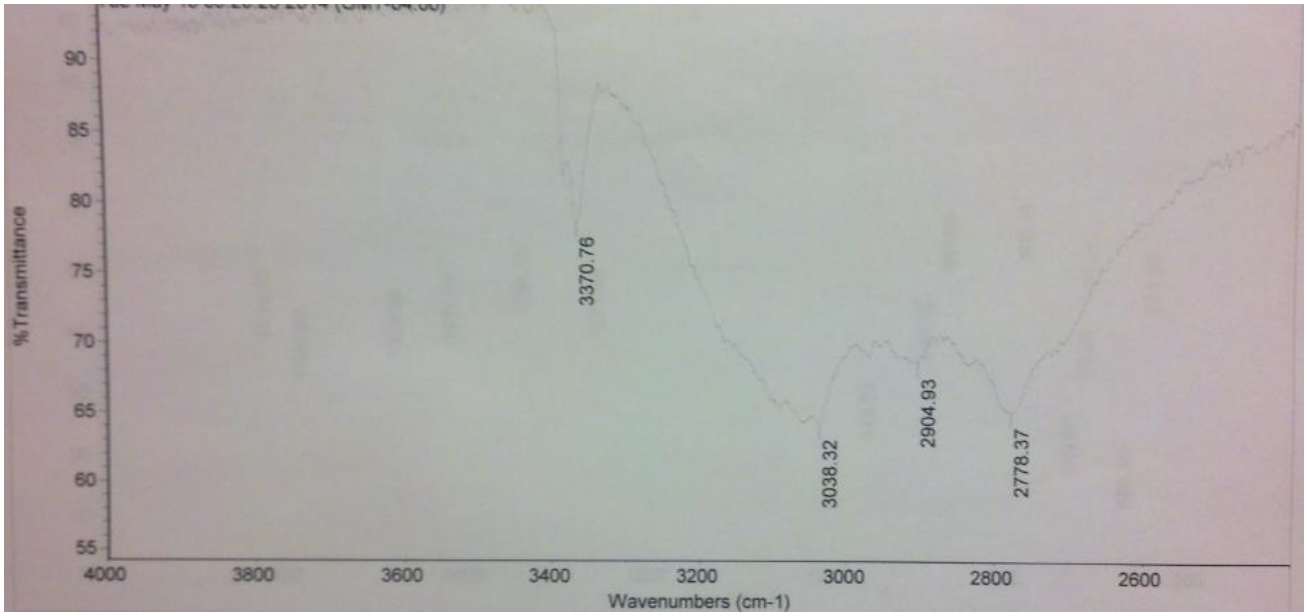

B

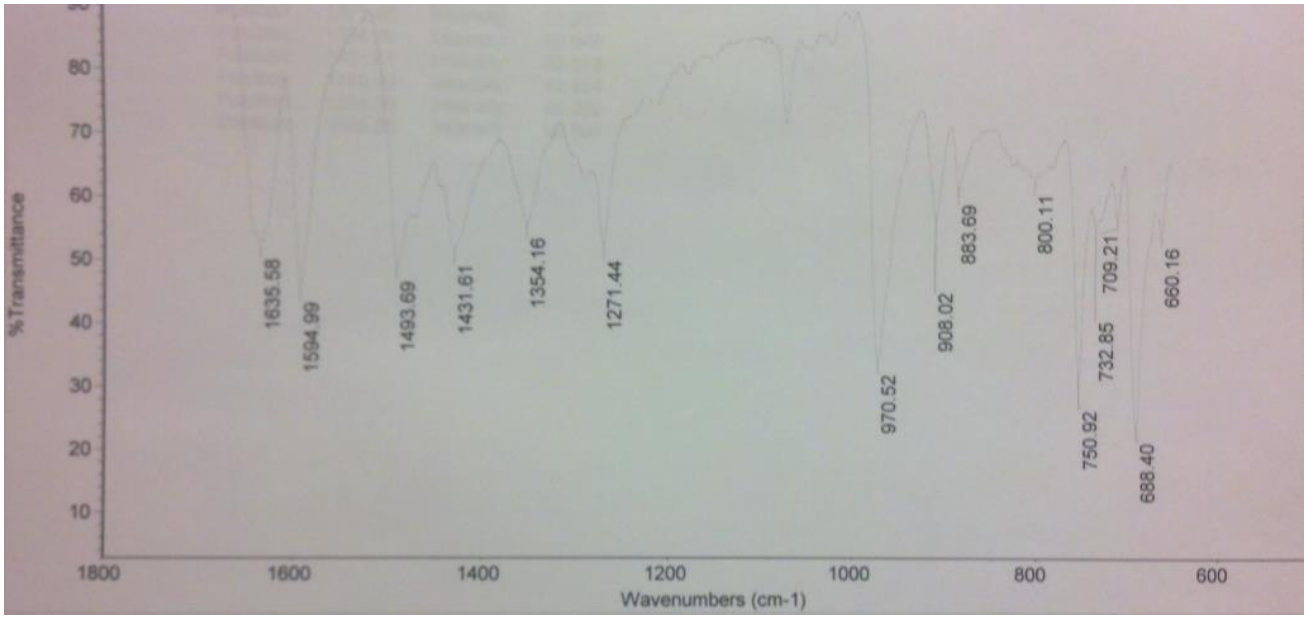

Compound C-3

A

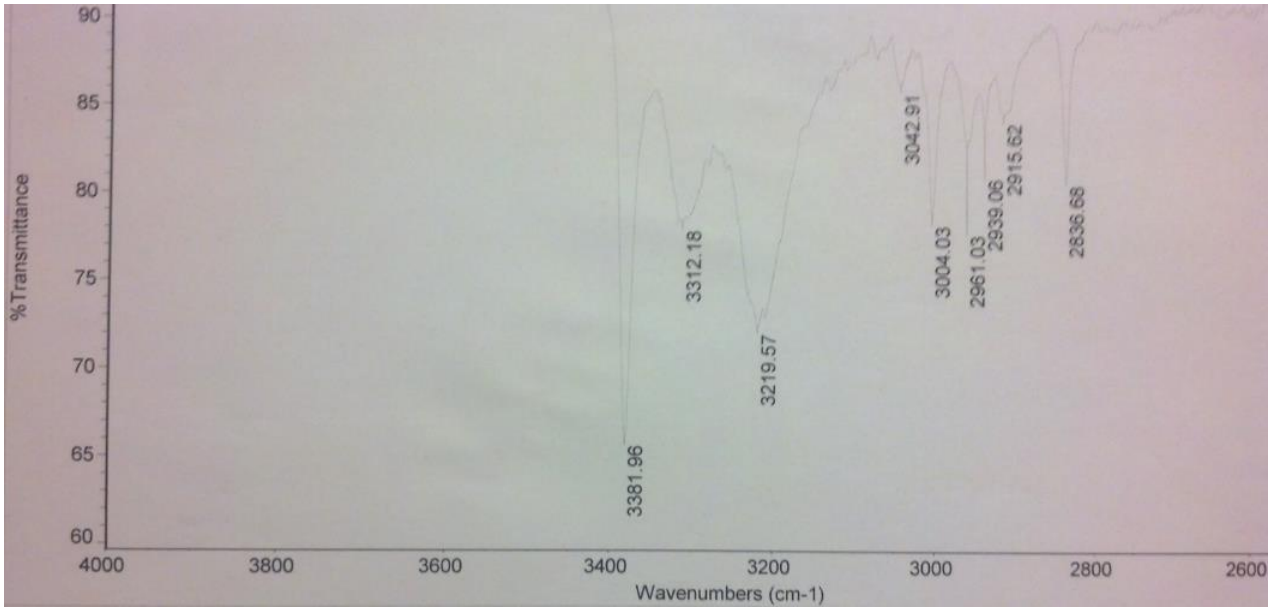

B

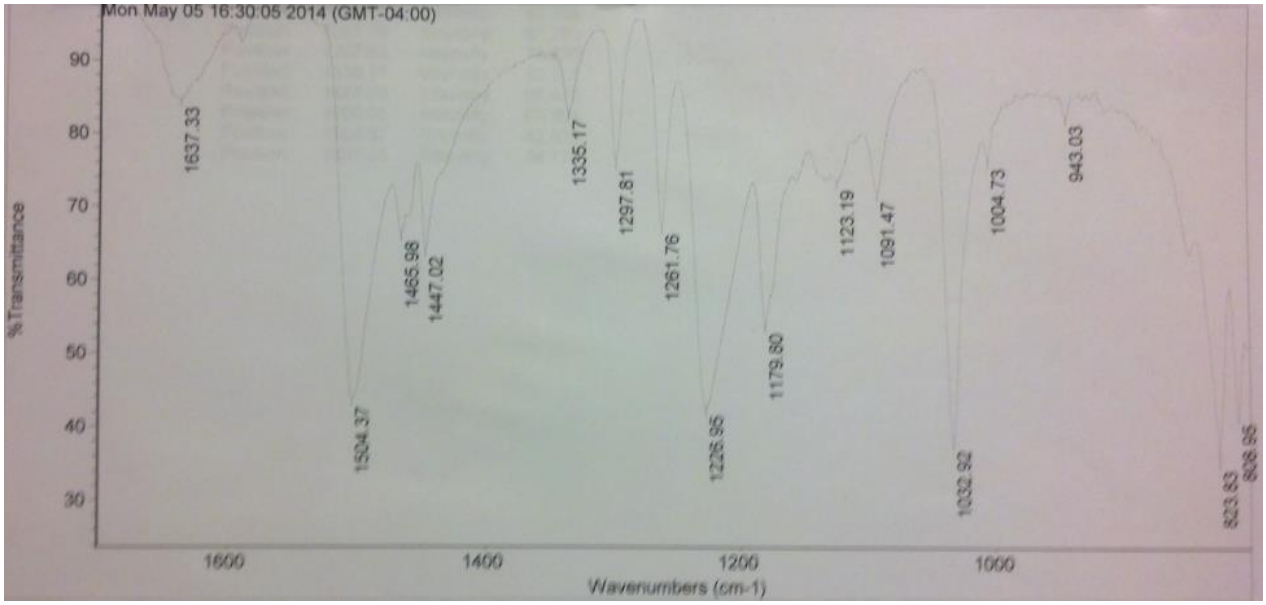

Compounds B-3 & D-3

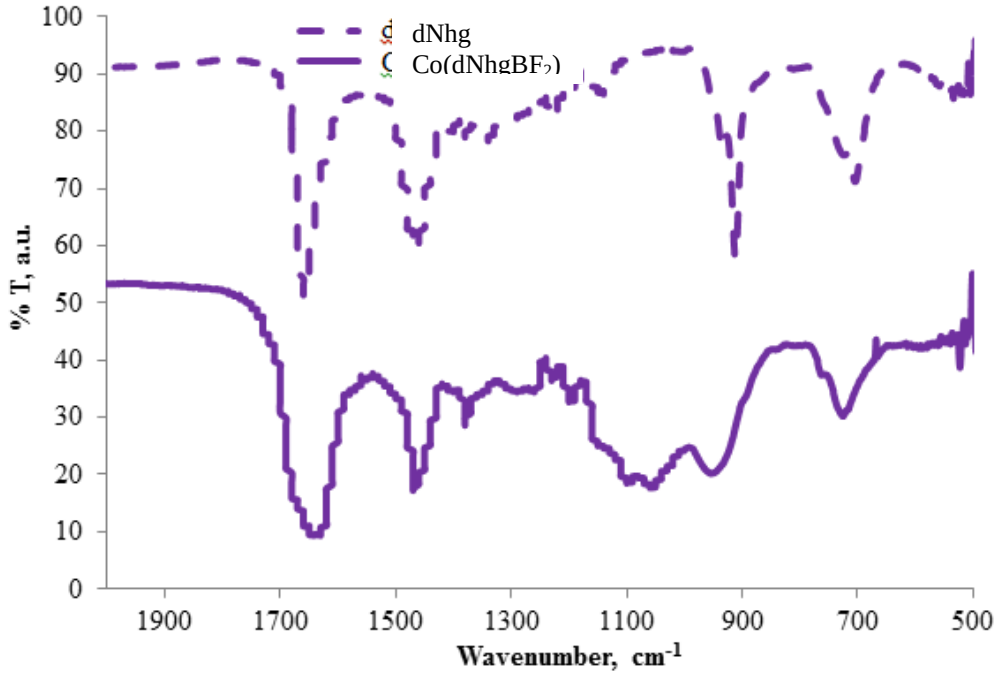

Appendix C – UV-visible spectroscopy data

Compound D-1 (green) and D-2 (blue) in acetonitrile

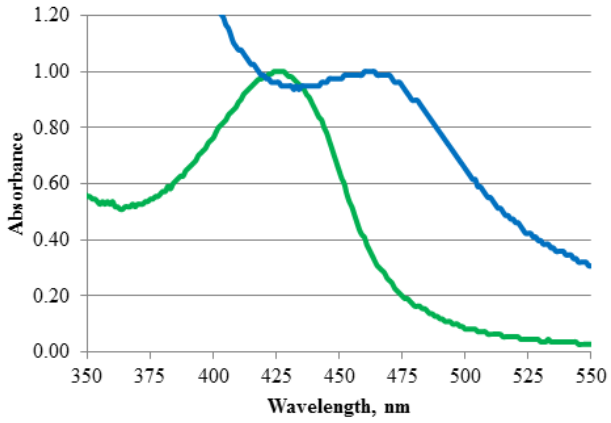

Compound D-3 in dichloromethane

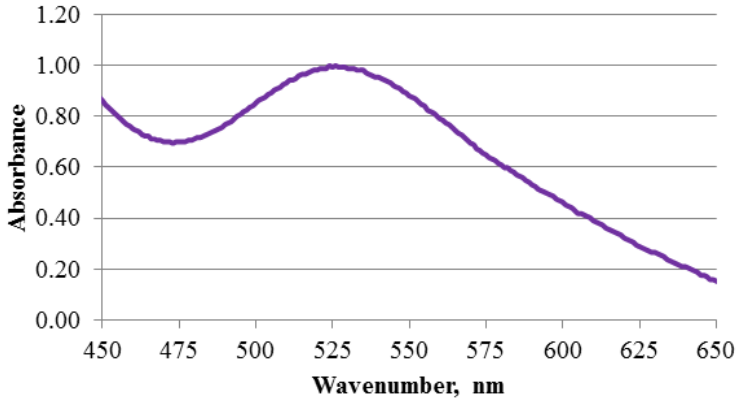

Compound D-4 in dichloromethane

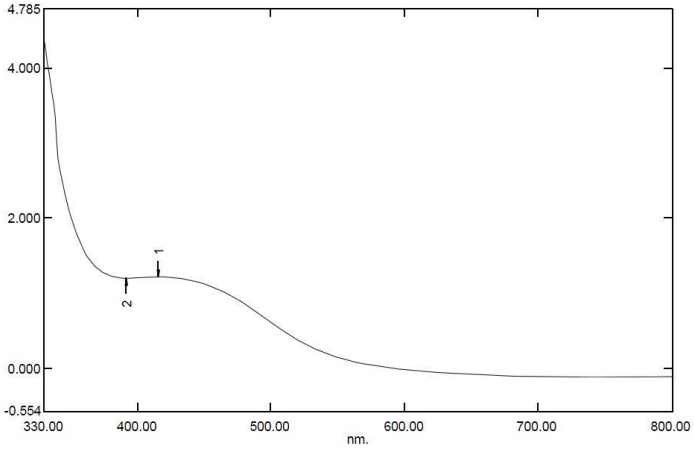

Appendix D – Cyclic Voltammetry

Cyclic voltammogram of D-3 in 0.1 M $TBAPF_6$ / dichloromethane solution. Glassy carbon working, Pt counter, Ag pseudoreference electrodes. Scan rates of 100 mV/s, 75 mV/s, and 50 mV/s. Deoxygenated by N_2. Red shows the $Co^{3+/2+}$ and black shows the $Co^{2+/1+}$ redox couple. Reproduced from reference 13.

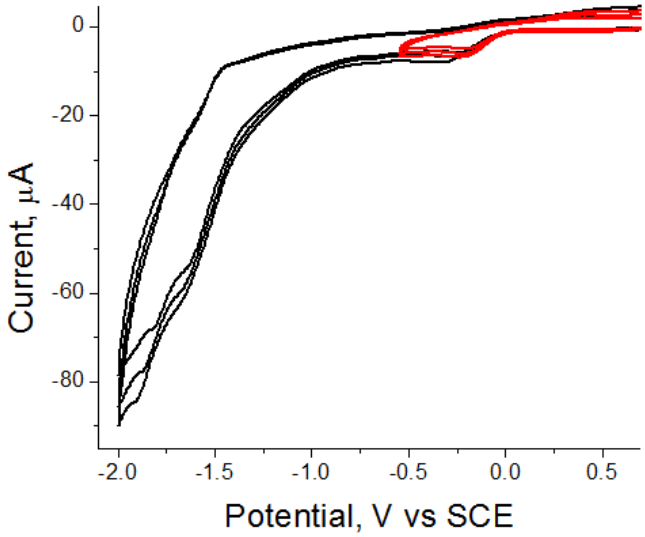

Cyclic voltammograms of D-3 with 0 mM to 6 mM of trifluoroacetic acid (TFA in figure) added in a solution of 0.1 M $TBAPF_6$ in dichloromethane. Glassy carbon working, Pt counter, Ag pseudoreference electrodes. Scan rate 100 mV/s. Deoxygenated by N_2.